MODELING AND CONTROL OF A STABILIZATION SYSTEM

KAMİL AFACAN

DECEMBER 2004

MODELING AND CONTROL OF A STABILIZATION SYSTEM

A THESIS SUBMITTED TO
THE GRADUATE SCHOOL OF NATURAL AND APPLIED SCIENCES
OF
MIDDLE EAST TECHNICAL UNIVERSITY

BY

KAMİL AFACAN

IN PARTIAL FULFILLMENT OF THE REQUIREMENTS
FOR
THE DEGREE OF MASTER OF SCIENCE
IN
MECHANICAL ENGINEERING

DECEMBER 2004

Approval of the Graduate School of Middle East Technical University

_____
Prof. Dr. Canan ÖZGEN
Director

I certify that this thesis satisfies all the requirements as a thesis for the degree of Master of Science.

_____
Prof. Dr. Kemal İDER
Head of Department

This is to certify that we have read this thesis and that in our opinion it is fully adequate, in scope and quality, as a thesis for the degree of Master of Science.

_____
Prof. Dr. Bülent Emre PLATİN
Co-Supervisor

_____
Prof. Dr. Tuna BALKAN
Supervisor

Examining Committee Members

Prof.Dr. Samim ÜNLÜSOY	(METU, ME)	_____
Prof.Dr. Tuna BALKAN	(METU, ME)	_____
Prof.Dr. Bülent Emre PLATİN	(METU, ME)	_____
Prof.Dr. Mehmet ÇALIŞKAN	(METU, ME)	_____
Burak GÜRCAN (M.Sc. in ME)	(ASELSAN)	_____

I hereby declare that all information in this document has been obtained and presented in accordance with academic rules and ethical conduct. I also declare that, as required by these rules and conduct, I have fully cited and referenced all material and results that are not original to this work.

Name, Last name : Kamil AFACAN

Signature :

ABSTRACT

MODELING AND CONTROL OF A STABILIZATION SYSTEM

Afacan, Kamil
M.S., Department of Mechanical Engineering
Supervisor : Prof. Dr. Tuna Balkan
Co-Supervisor: Prof. Dr. Bülent Emre Platin

December 2004, 76 pages

Elevation axis model of a barrel stabilization system is constructed. The nonlinearities which are considered in the model are orifice flow characteristics, coulomb friction, hard-stop limits, kinematics of the system and unbalance on the barrel. A Simulink® model for the servo valve, actuation system and barrel is constructed. Servo valve identification is made via the actual test data. Compressibility of the hydraulic fluid is taken into consideration while modeling the actuation system. Friction model is simulated for different cases. Controller of the system is constructed by two PIDs, one for each of the velocity and the position loops. Velocity feed forward can reduce the time to make a quick move by the system. The disturbance is evaluated from a given road profile and disturbance feed forward is applied to the system.

Keywords : Barrel Stabilization, Servo Valve Model, Friction Model, Disturbance Feed Forward

ÖZ

BİR STABİLİZASYON SİSTEMİNİN MODELLENMESİ VE KONTROLU

Afacan, Kamil
Yüksek Lisans, Makine Mühendisliği Bölümü
Tez Yöneticisi : Prof. Dr. Tuna Balkan
Ortak Tez Yöneticisi : Prof. Dr. Bülent Emre Platin

Aralık 2004, 76 sayfa

Bir namlu stabilizasyon sisteminin irtifa eksen modeli yapılmıştır. Sistem modellenirken karşılaşılan ve modele dahil edilen nonlineer bileşenler şöyle sıralanabilir: Akış karakteristiği, Coulomb sürtünmesi, mekanik sınırlayıcılar, sistemin kinematik yapısı ve namlunun kütle merkezi kaçıklığı. Servo valfin, tahrik sisteminin ve namlunun modelleri Simulink® ortamında yapılmıştır. Servo valf geçek test bilgileri kullanılarak tanımlanmıştır. Tahrik sistemi modellenirken hidrolik akışkanın sıkıştırılabilirliği dikkate alınmıştır. Sürtünme modeli değişik durumlar için koşturulmuştur. Sistemin denetimi temel olarak 2 PID'den oluþmaktadýr. Biri konumu diðeri hýzý kontrol etmektedir. Sistemin ani hareket yapmasý için gereken zamaný azaltmak için hýz isteði ileri beslemesi yapýlmýþtýr. Bozucu sinyal belirlenen yol profilinden hesaplanmýþ ve bozucu sinyalin sisteme bildirimi gerçekleþtirilmiþtir.

Anahtar Kelime : Namlu Stabilizasyonu, Servo Valf Model, Sürtünme Modeli, Bozucu Ýleri Besleme

ACKNOWLEDGMENTS

The author wishes to express his deepest gratitude to his supervisor, Prof. Dr. Tuna Balkan and co-supervisor Prof. Dr. Bülent Emre Platin, for their guidance, advice, criticism and encouragement and insight throughout the research.

The author is also grateful to Prof. Dr. Kemal Özgören, Prof. Dr. Mehmet Çalışkan, Mr. Burak GÜRCAN and Asst. Kerem ALTUN for their suggestions and comments.

This study was supported by Turkish Naval Forces.

The author also would like to thank his wife Seda and his parents, for their encouragement and patience.

TABLE OF CONTENTS

PLAGIARISM iii
ABSTRACT iv
ÖZ v
ACKNOWLEDGEMENTS vi
TABLE OF CONTENTS vii
LIST OF TABLES ix
LIST OF FIGURES x
CHAPTERS
1. INTRODUCTION 1
1.1. Stabilization of Barrel on a Main Battle Tank 2
1.2. Aims of the Study 6
1.3. Scope of the Study 7
2. SYSTEM MODELING 9
2.1. System Model 10
2.2. Servo Valve Model 12
2.2.1. System Identification 15
2.2.2. Load Pressure Feedback 19
2.2.3. Dither Signal 20
2.3 Actuator Model 21
2.4. Barrel Model 25
2.4.1. Unbalance Effect 30
3. CONTROL STRATEGIES FOR DISTURBANCE REJECTION 34
3.1. Controller 34
3.2. Disturbance Feed Forward 35
3.3. Feed Forward in Velocity Loops 41
4. SIMULATION 42
4.1. Valve Model and Identification Results 42
4.1.1. Valve Identification Results 45

4.2. Actuator Model 47
4.3. Friction Test Results 48
4.4. Barrel Model 52
4.5. System Simulation 53
5. CONCLUSION 64
5.1. Summary and Conclusion 64
5.2. Recommendations for Future Work 66
REFERENCES 67
APPENDICES 69

LIST OF TABLES

Table 1 Frequency Response Data 37
Table 2 PID Parameters used in the Simulations.....56

LIST OF FIGURES

Figure 1. Barrel Motion with and without Stabilization System, in Elevation 2
Figure 2. Barrel Motion with and without Stabilization System, in Azimuth 3
Figure 3. Closed Loop Servo for Basic System for one axis 4
Figure 4. Second Generation Stabilization System for one axis 4
Figure 5. Schematic View of Valve, Actuator and Barrel 10
Figure 6. Block Diagram Representation of Barrel 11
Figure 7. Schematic Representation of Servo Valve Block 12
Figure 8. Displacement Axis and Flows in Servo Valve 13
Figure 9. Three Stage Servo Valve Block Diagram 13
Figure 10. Servo Valve Illustration 14
Figure 11. Block Diagram of the Servo Valve Model 15
Figure 12. Input Signal of Servo Valve for System Identification 17
Figure 13. The LVDT Output of Servo Valve Test 17
Figure 14. Servo Valve Spool Step Responses for Different Input Values 18
Figure 15. Double Acting Type Actuator 21
Figure 16. Causality Block Diagram of Flow Rate and Pressure 23
Figure 17. Barrel and Actuation (Slider Crank) Mechanism 23
Figure 18. Torques acting on the Barrel 25
Figure 19. Coulomb + Viscous Friction Characteristics 27
Figure 20. Simplified View of the Barrel Joint 28
Figure 21. Flow Chart of Barrel Movement According to the Friction 29
Figure 22. Unbalance Effect on the Barrel 30
Figure 23. Instantaneous Center of Rotation and Normal Acceleration 31
Figure 24. Angular Displacement on Road Profile 32
Figure 25. Classical Control Algorithm 35
Figure 26. Feedback System with Disturbance Input 35

Figure 27. Feedback System with Disturbance Feed Forward 36
Figure 28. Bode Plot of Plant's and Disturbance Transfer Functions.... 38
Figure 29. Bode Plot of the Disturbance and the Plant and the Identifications..... 39
Figure 30. Bode Plot of the Disturbance Feed Forward Transfer Function..... 40
Figure 31. Velocity FF in Controller..... 41
Figure 32. First Stage of the Servo Valve Model 42
Figure 33. Flow Characteristics Model of the Servo Valve..... 43
Figure 34. Servo Valve Model..... 45
Figure 35. Error Surface for Servo Valve Identification..... 46
Figure 36. Servo Valve Simulation and Experiment Comparison 46
Figure 37. Inverse Kinematics of Slider-Crank Mechanism 47
Figure 38. Actuator Model in Simulink 48
Figure 39. Velocity and the Position of Simplified Barrel..... 49
Figure 40. Friction Model 50
Figure 41. Velocity and the Position of Simplified Barrel..... 51
Figure 42. Velocity and the Position of Simplified Barrel..... 51
Figure 43. Friction and End-Stop Logic Block in Barrel Model..... 52
Figure 44. Controller of the System 53
Figure 45. Controller of the System with Velocity FF 54
Figure 46. Barrel Dynamics Model..... 54
Figure 47. Step Response of the System 55
Figure 48. Comparison of the Responses for Different Velocity FF Gains 56
Figure 49. Zoomed View of Figure 48..... 57
Figure 50. Barrel Stabilization System..... 58
Figure 51. Road Profile..... 59
Figure 52. Disturbance and Effect Disturbance FF with a Velocity of V=20 km/h 59
Figure 53. Zoomed View of Figure 52..... 60

Figure 54. Position of the Barrel with Disturbance FF with a Velocity of V=20 km/h 60
Figure 55. Zoomed View of Figure 54..... 61
Figure 56. Disturbance and Effect Disturbance FF with a Velocity of V=40 km/h 61
Figure 57. Zoomed View of Figure 56..... 62
Figure 58. Position of the Barrel with Disturbance FF with a Velocity of V=40 km/h 62
Figure 59. Zoomed View of Figure 58..... 63

CHAPTER 1

INTRODUCTION

Weapons used in the battlefield are demanded to be lighter, more mobile, easily controllable and able to shoot with a high accuracy. One of these weapons used in land is the Main Battle Tank (MBT). MBT is probably the most important weapon because of its being mobile, armored and having heavy-fire capacity. Developments of MBT are parallel to the improvements in heavy weaponry, Weapon Control Systems (WCS) and hull mobility. Heavy weapons have became more effective with the improvements in material science and chemistry. Mounting of these weapons to the hull produces some problems. Control systems become more important while the system become larger and more complex. Drive technology and control systems determine the size of the MBT. Hull mobility depends on the vehicle technology to overcome the problems of cross-country movement.

Mobility demands in battlefield lead to the requirement of firing while moving instead of stopping at each time the MBT engages a target. This demand can be achieved by WCS by minimizing the tank's hull movement effects on the barrel.

In early tanks used in World War I, free elevation type of mounting was used and it was controlled by a shoulder strap. As the weapons got heavier this control became impossible and changed with manually operated gears. Up to 1940's this situation continued. The disadvantages of this setup are the insufficiently precise control, more human power and very low speed while steering the barrel. This is followed by the use of hydraulic drive systems. After electrical motors were used for slewing the barrel, rapid and precise control has been satisfied. Improvements in traversing the turret were

applied to the powered control of the elevation control of tank guns. This adoption has led to the stabilization of the barrel [1].

1.1 Stabilization of Barrel on a Main Battle Tank

Motion of vehicles causes some unwanted movements on the barrel. These movements must be minimized in order to hit a target while moving. Gunners are expected to minimize this effect especially in elevation by rotating the barrel in the opposite direction of the hull's motion. But the frequency of this kind of motion varies from 0 to 3-4 Hz while the response of the human operators is not more than 0.5 Hz [2].

In this situation, the effects of vehicle motion on the barrel can be minimized by stabilization systems which are designed to maintain the barrel position according to the earth. Figure 1 and Figure 2 illustrate the problem in detail [1].

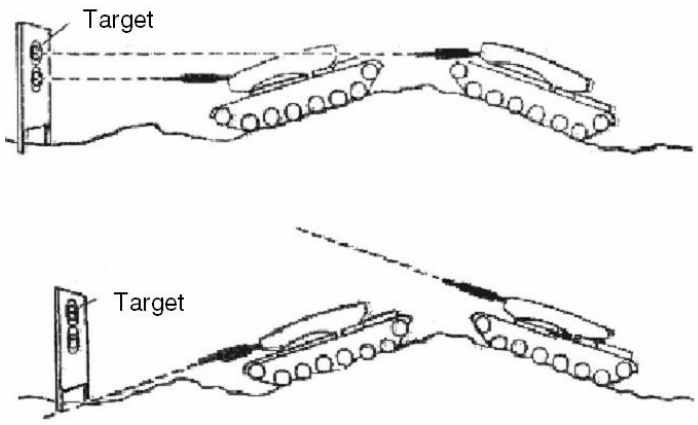

Figure 1. Barrel Motion with and without Stabilization System, in Elevation

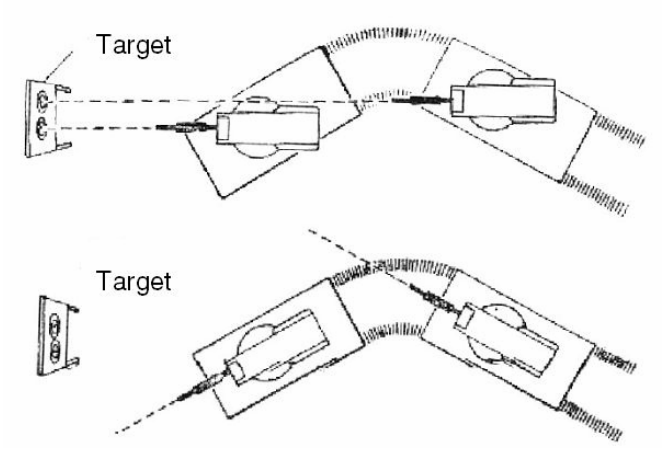

Figure 2. Barrel Motion with and without Stabilization System, in Azimuth

Systems aimed to do this stabilization basically closed loop servo systems which control the movement of the barrel relative to the earth by using gyroscopes and feedback signals produced by them.

Simplest stabilization systems are assigned to cope with the elevation changes and made up of a single closed loop system with a rate gyroscope mounted on the barrel to sense its angular velocity.

The "*basic systems*" involve two closed-loop servo systems, one for the elevation and the other for the azimuth axis of the gun. Each loop contains a gyroscope to sense the velocities in respective axis (Figure 3). Any difference between the sensed and the commanded velocities by the operator, cause to start the servo motors to nullify the error, hence to stabilize the turret. This type of two axes stabilization systems were developed during World War II.

Two axis control systems are proved to be effective, but it was not easy for the operators to correct the stabilization errors and the systems were not

rapid enough to reduce the pointing errors to a sufficiently low level while the tank moves on a rough terrain.

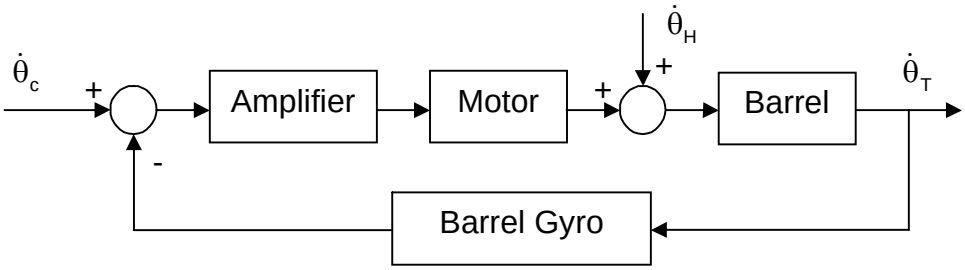

Figure 3. Closed Loop Servo for Basic System for one axis [2]

This led to the "*second-generation*" control systems in early sixties. These systems contain two extra gyros which feed the tank's movement forward in the system to make the turret more sensitive and rapid against the tank's movement (Figure 4). This method improved the stabilization of the guns. Second generation lowers the error by 50 % of the error in basic systems [3].

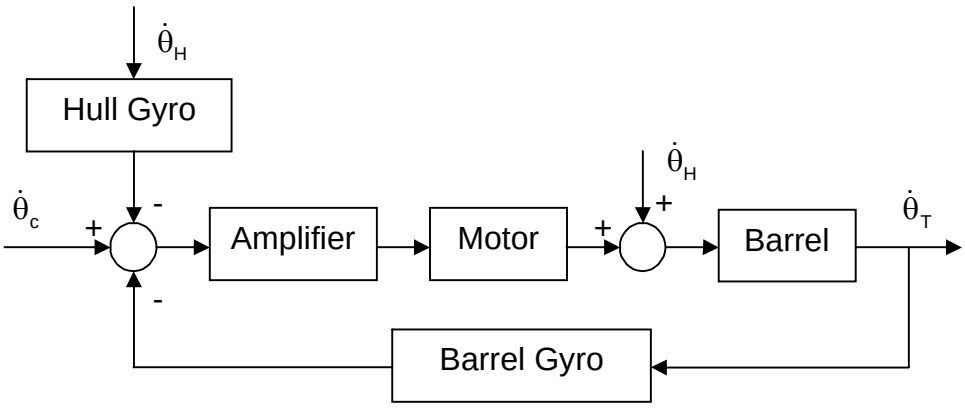

Figure 4. Second Generation Stabilization System for one axis [2]

To provide appropriate feed forward signals two gyroscopes are mounted one to the hull and the other to the barrel. The use of the feed forward control was pioneered by the Cadillac Cage Company in the late 1950s. This stabilization system was demonstrated in 1962 and firstly adopted to the Leopard I Tanks in 1969-1970 by German and Belgian Armies. Feed forward control application was seen in Soviet Army with a difference from the others. The stabilization systems include rate integrating gyros which provide a memory for the barrel position. So the barrel can be driven to the old position just before the disturbance.

"Director-type" system based on the independently stabilized gunner's sight was first developed in 1960s by the Delco Electronic Divisions of General Motors. Chrysler version of this system stabilized position of the gun only in elevation. A simpler alternative to this system was developed by Bofors Aerotronics in Sweden and by Marconi Command and Control Systems in England in the form of a pseudo-director system. The advantage of this system is that it provides a highly stabilized aiming mark without the complexity of an independently stabilized sight and can be applied readily to existing tanks with simple telescopic or periscopic sights mechanically linked to tank guns. In fact, Bofors Aerotronics produced this system, from 1983 onwards, for Centurion tanks. But it does nothing to improve the stability of the image which the gunner sees.

Another refinement is the introduction of rate-aided tracking. This represents an advance on the compensation of the angular motion of tanks. Although a rate-aided tracking is added, the gunner has to compensate for any changes in motion of the target [2,3]. Nevertheless, it improves the performance. Delco Electronics produced and used this in Leopard 2, which became the first tank to go into service.

Hence the barrel stabilization is mostly related to military and defense and it is treated as classified and therefore its details are not available in open literature. Some of the studies about this subject can be listed as follows.

In 1984, Balaman is studied the control of a manipulator with two angular degrees of freedom. This study is dealed with modeling and optimization of the system. It does not include the friction [4].

In 1998, Purdy enhanced the stabilization ratio by using the hull rate gyroscope for feed forward. This study gave the results of the simulations of linear and nonlinear model with and without disturbance feed forward and nonlinear model with feed forward and friction compensation [5]. In another study in 1999, Purdy made a simple elevation model and examined the out of balance effect on WCS [6]. These studies deal about the electrical drive technology. They also have no model in a computer program revealed in the publications.

A stabilization and hull model is developed by Şahin in 2001. In this study all the system elements were assumed to be linear. Stabilization was tried to be satisfied with the controller. There was no disturbance feed forward to stabilize the system [1].

1.2 Aims of the Study

In this study, the stabilization of the barrel on a MBT in elevation axis is considered. Only the elevation axis is considered because it is affected much more than the azimuth axis from the road profile. Since a stabilization system improve an ability of hitting targets while the tank is moving without stopping, the effects of disturbances on the barrel should be taken into account.

Unbalance caused by mounting the barrel off center of mass, friction at joint, hydraulic actuator as the driving unit and control system are the causes of using a stabilization system. In this study, all of these components are modeled and simulated under specified conditions.

The brain of the stabilization system is the controller. PID controllers are used to control the position and the velocity of the system. To be able to tune the parameters of the controller, either an experimental setup should be used or a model should be constructed. The use of experimental setup may cause trouble and may be dangerous for the setup. To prevent from these undesired situations such as damaging the system elements, operator injury etc., a model will be constructed and controller parameter tuning and system modifications will be realized by using this model.

Finally, the whole system or the elements of it can be used for other design and modernization studies.

1.3 Scope of the Study

It is intended in the study to model the elevation axis of a barrel completely in Simulink® 5.0 in Matlab® 6.5 environment and simulate the disturbance effects on it. This model includes barrel, hydraulic actuator as driving unit, an electro-hydraulic servo valve to manipulate the actuator and a controller unit.

In Chapter 2, the system elements are modeled and assumptions made while modeling are noticed for every element.

The properties of the servo valve used to control flow are explained. A system identification is made for the servo valve by using its experimental test outputs to determine the valve gain and the time constant. The nonlinear flow characteristics of the servo valve are derived and modeled.

The actuation system as a slider-crank mechanism is modeled. Inverse kinematics is used to solve the relation between the barrel's angular position and the actuator position while the motion is transformed from translational movement to rotational.

There are a lot of parameters which define the barrel's motion such as frictions in the barrel joint, the compressibility of the hydraulic fluid, unbalance caused from mounting point of the barrel to the hull and inertia.

The controller is made up of two PID's one for each loop feeding back the velocity and the position of the barrel.

In Chapter 3, some possible stabilization strategies are discussed. The disturbance caused by the road and transferred over the hull is modeled. The stabilization method to overcome the disturbance which can be measured by means of gyroscopes is examined.

Two tests with fixed velocity at 20 km/h and 40 km/h are realized for an assumed road profile. Parameters and results are introduced in Chapter 4.

Finally, Chapter 5 discusses about the results and conclusions of the study.

CHAPTER 2

SYSTEM MODELING

Modeling is the starting point of design, production, test and control. A good modeling will settle most of the problems in the design step. Also in the production case, modeling will help to define many of the criteria. The test and control stages are also critical. Because of many restrictions, the control and the test stages are realized in a tight manner. On the other hand with a well designed model, tests can be made on the model without any damage risk to the system. All critical values can be tested and determined in this way. This will also give a chance to determine the limits of the system approximately proportional to the accuracy of the model. It can be helpful to select the controller parameters for the system. In all of these cases, the model shows its effect on the situation.

While modeling, it should not be forgotten that the more the properties introduced to the model the more the problems occur. If all the parameters of the real system were tried to be included in the model, this would probably generate many problems such as the increase in the number of the logical operators, time spent for the evaluation, solver errors caused by the time step and more computer capabilities need etc. All of the real world can not be modeled in the same way. Sometimes modeling so many details becomes harmful instead of being helpful as the system may not be settled with the desired accuracy because of the problems mentioned above. While modeling, critical case is to determine the modeling criteria and assumptions.

While constructing the elevation axis model, the following assumptions are made:

- There is a stable source of hydraulic fluid supply at constant pressure.
- Effects of hydraulic fluid inertia are negligible.
- Gage pressures are used.
- No temperature change exists.
- There is no leakage.

2.1. System Model

In this study, the *"system"* will represent the union of the servo valve, the actuator and the barrel as seen in Figure 5. Hull dynamics is not included in the system mentioned in this study. While it is assumed that road profile is known and correctly transformed via the gyroscopes on the hull, it is included in the system as disturbance representing the hull motion. As the hull dynamics is not modeled here, all the inputs to the elevation axis model are accepted as the outputs of the hull dynamics directly.

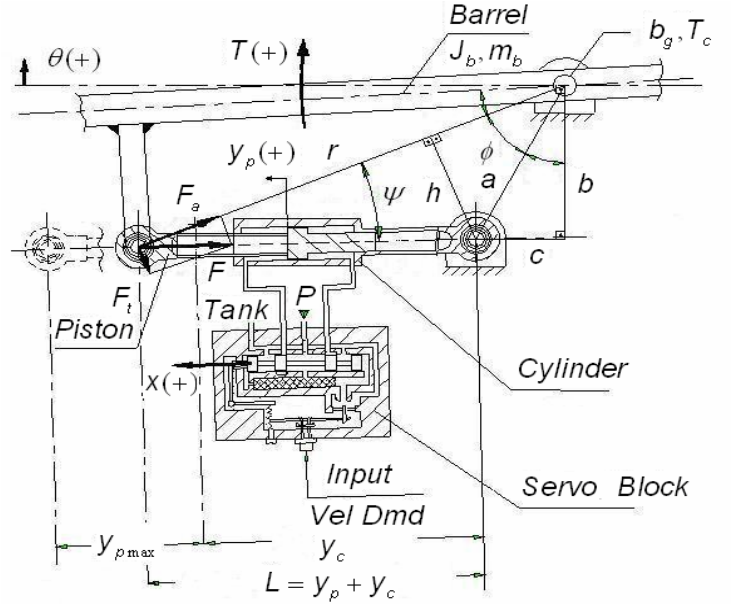

Figure 5. Schematic View of Valve, Actuator and Barrel (Adopted from [7])

The nomenclature used in Figure 5 is as follows.

T	:	Torque created by tangential force of the actuator component
J_b	:	Inertia of barrel
m_b	:	Barrel mass
x	:	Servo valve position
y_p	:	Stroke
y_c	:	Cylinder closed length
b_g	:	Viscous friction at barrel mounting
T_c	:	Static friction torque at barrel mounting
F	:	Force produced by actuator
F_t	:	Tangential force
θ	:	Angular position of barrel
P	:	Hydraulic fluid supply
L	:	Length of the stroke with cylinder closed length

Whole system is drawn as a block diagram in Figure 6.

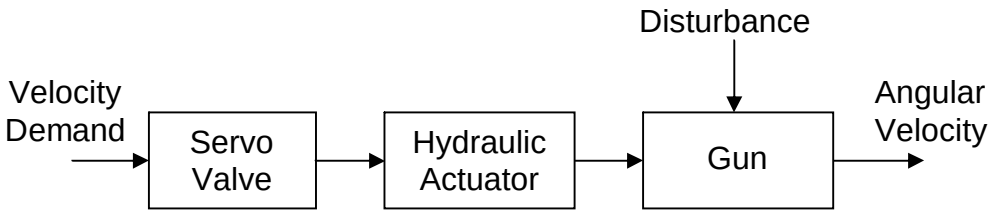

Figure 6. Block Diagram Representation of Barrel

Input of the system is the velocity command to the servo valve. The working fluid transports its energy to the actuator to be able to overcome the friction,

move and stabilize the barrel at a demanded velocity with a desired accuracy.

2.2. Servo Valve Model

A classical four way, zero-lapped valve is used to excite the actuator. The servo valve has 3 stages; flapper as first, spools as second and third stages. A schematic representation of the valve used in this study is seen in Figure 7.

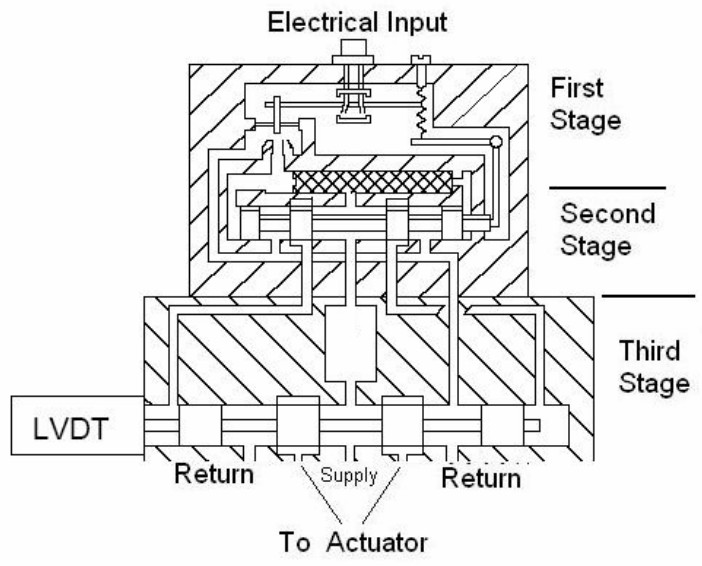

Figure 7. Schematic Representation of Servo Valve Block [7]

The first stage is an electrically driven flapper nozzle type. The flapper moves by the force generated from the induction of two coils by DC current. In the first stage the input is the current and the output is the flapper position. The flow characteristics is nonlinear but there is no chance to determine the position and the exact flow. By assuming that the force acting on the spool caused by the pressure in the chamber is proportional to the

flapper position, it can be illustrated by a constant which will be the gain of the transfer function between the flapper and the spool position. In second stage, the input is the flapper position and the output is the spool position. In this case, also there is no chance to determine the position of the spool and the exact flow. At the third stage the position of the second stage spool is the input and third stage spool position is the output. Displacements and flows are indicated in Figure 8.

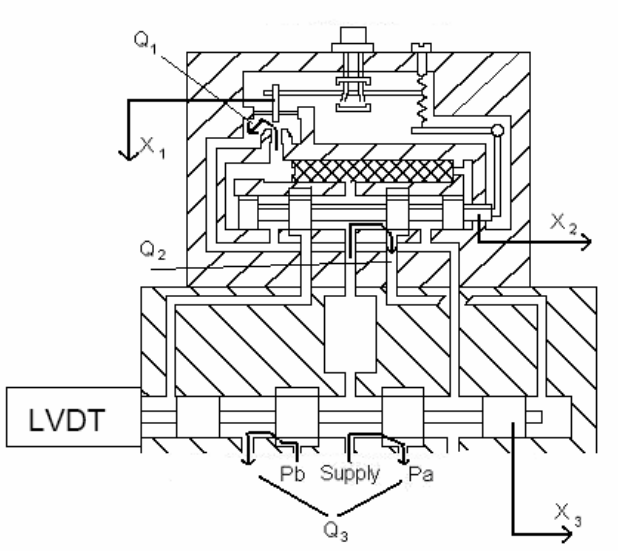

Figure 8. Displacement Axis and Flows in Servo Valve (Adopted from [7])

The block diagram of this servo valve will be as follows.

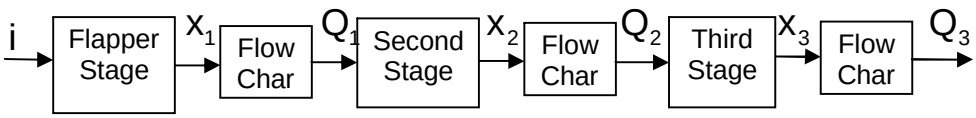

Figure 9. Three Stage Servo Valve Block Diagram

But a modeling servo valve as seen in Figure 9 is almost impossible while the parameters like mass, friction and stiffness of the stages separately are unknown. There is no chance to make individual tests for each stages of the valve. But, it is possible to determine the overall characteristics of the valve considering all three stages together. In these tests realized in ASELSAN just Linear Variable Differential Transducer (LVDT) outputs can be measured and recorded. LVDT is a device which determines the position of the spool and produce electrical signal proportional to this position. Because of these difficulties, the model of the valve can be modified as seen in Figure 10.

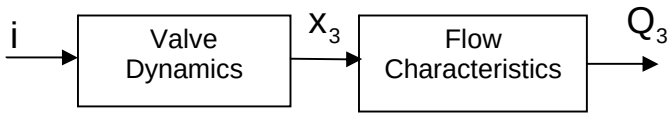

Figure 10. Servo Valve Illustration

In this block diagram, valve dynamics represents all three stages together. While the parameters of the electrical stages can not be evaluated, only the nonlinearity in the third stage is taken into account and the rest of the system is included in the transfer function of the plant. The output of the LVDT is measured and the flow rate is calculated from this value via orifice equation.

$$Q = C_d w x_3 \sqrt{\frac{2}{\rho}(p_1 - p_2)} \qquad (2.1)$$

where;

Q : Volumetric flow rate

C_d : Orifice discharge coefficient

w : Width of the orifice inlet

ρ : Density of working fluid

p_1 : Pressure at inlet of the orifice

p_2 : Pressure at the exit of the orifice

x_3 : The position of the third stage

For the dynamic characteristics of the valve, a second order transfer function can be used which represents a mass with friction. If this transfer function and (2.1) is substituted in Figure 10, block diagram of the servo valve can be drawn as shown in Figure 11.

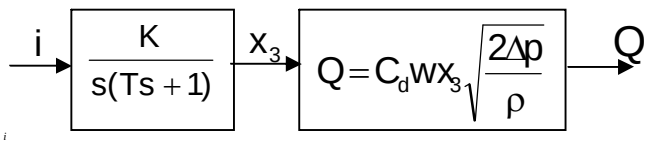

Figure 11. Block Diagram of the Servo Valve Model

Here are the assumptions made while modeling the servo valve.

- Temperature change in the fluid is neglected.
- Valve case is absolutely rigid.
- Compressibility of the hydraulic fluid is negligible because valve chambers are too small comparing to the volumes of the actuator chambers.
- Both spools are zero-lapped.
- There is no internal leakage in the valve.

2.2.1 System Identification

Computer simulations of systems give the opportunity to the users to study

on the computer to make the design instead of constructing real systems. Thus less money and time will be spent for this job. While simulating these systems, all of the possible system parameters are tried to be illustrated in computer to determine a better starting point to the design case. But it should not be expected that the response of the simulations will be the same as the real system even parameters of the real system are known. On the other hand, there are a lot of systems for which the parameters can not be determined while there will be no chance to examine the elements of the system individually and measurement device capability and the accuracy will be effective. These kinds of system need to be identified.

Matlab® and similar programs introduce us many methods to identify the systems. System Identification Toolbox is one of these opportunities. But in this study, instead of using these methods in Matlab®, a cost function which is defined as follows, will be minimized for identifying the servo valve parameters.

$$J = \sum_{k=1}^{n} (y_m - y_t)^2 \quad ; \quad k=1,2,\ldots..,n \tag{2.2}$$

where;

J	:	Cost function
y_m	:	Model output
y_t	:	Test output
n	:	Number of the samples

Servo valve used in the elevation axis model is identified in [7] with MATLAB® System Identification Toolbox®. The servo valve was excited with a square wave which had a changing amplitude so that different magnitude step responses were obtained as seen in Figure 12.

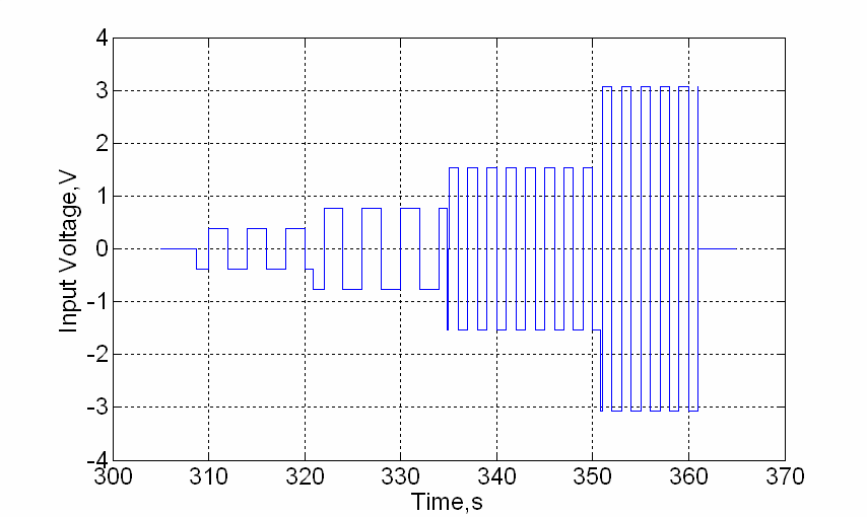

Figure 12. Input Signal of Servo Valve for System Identification [7]

The position of the spool was determined by a LVDT and recorded as the output. Making these tests at different amplitudes gave more information about the valve characteristics. The output plots can be seen in Figure 13. The valve was controlled by a PID while the position of the third stage spool (LVDT) is fed back [7].

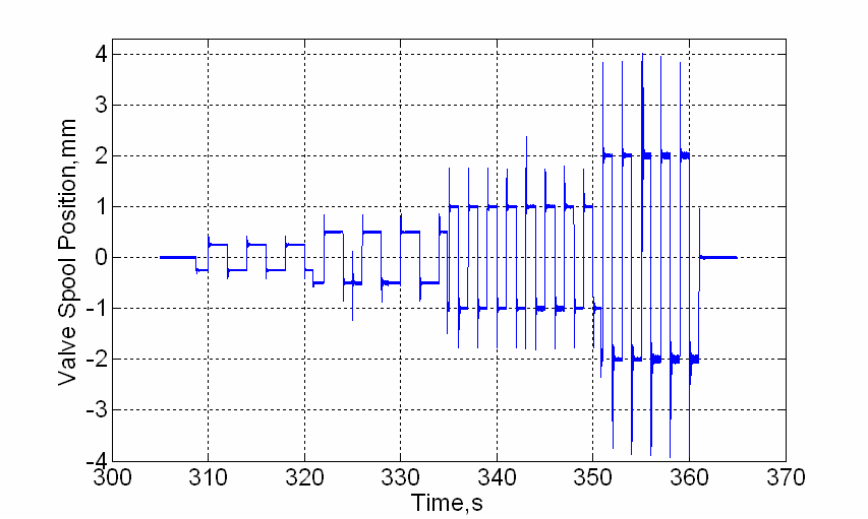

Figure 13. The LVDT Output of Servo Valve Test [7]

But this identification is made between the command input which is an electrical signal and the position of the valve in mm. In this study, this identification is repeated while taking the input as the position demand corresponding to the electrical input in mm.

As seen in Figure 13 there are transition periods and some disturbances which can not be used in identification. By omitting the transient periods and extraordinary fluctuations, step responses are obtained and plotted on the same graph in Figure 14 for one second duration, which is an enough period for settling.

A valve model which has the transfer function seen in Figure 11 is constructed. In this model, two parameters are tried to be determined, time constant,T of the valve and the valve gain,K. The time step is taken same as the test environment and sampling rate of the output data, $1x10^{-3}$ sec. These two parameters are determined via an “m” file with direct search method and cost function values are recorded in an error matrix.

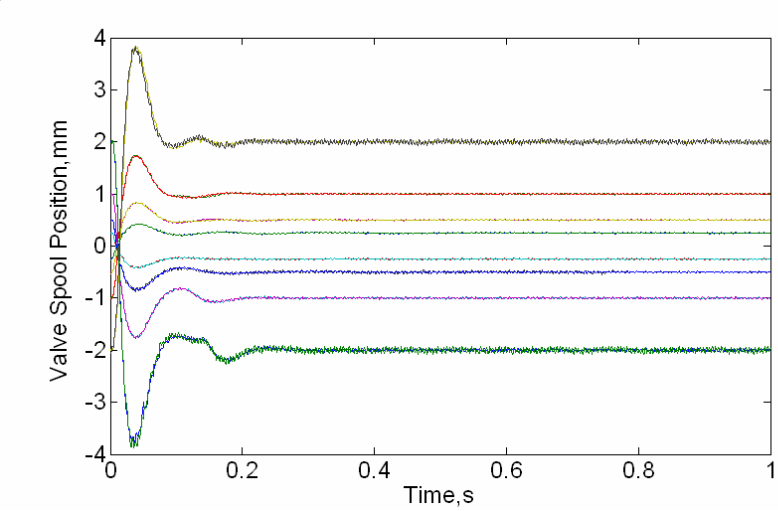

Figure 14. Servo Valve Spool Step Responses for Different Input Values

As can be seen in Figure 14, valve step responses differ from each other. Valve shows different dynamic behaviors at different amplitudes. In this situation, although identification will fit exactly to one of the step response, it would not be the optimum solution for the other magnitudes. Thus, the solution differs also at each amplitude. Anyone of the valve gain and time constant pairs for these step responses could not represent all of the step responses with the same accuracy. “m” files used in the simulations and calculation is given in Appendix 1.

Until now, the transfer function between the position command and the spool position is determined. The nonlinearity in the valve is maintained by using the orifice equation (2.1) to derive the flow from the valve.

2.2.2 Load Pressure Feedback

The servo valve is used to control the velocity of the actuator. Pressure feedback is a way of adding damping to this subsystem. Pressure feedback is able to increase damping based on the fact that the cylinder pressure is related to the derivative of the cylinder velocity. Feeding back the derivative of the cylinder velocity increases the damping of the system, thus improves the transient performance. The only problem with this strategy is that the pressure information also contains the effect of external forces. A high-pass pressure filter is introduced to deal with this problem. The form of the compensator is shown in equation (2.3) [8].

$$G_{HP} = \frac{\tau s}{\tau s + 1} \tag{2.3}$$

The τ value can be set through a wide range. Mostly, this parameter is selected for each specific system application separately and influenced by various system requirements such as system frequency, response and

stiffness. τ generally corresponds to a corner frequency of about 1/3 of resonant load frequency, f_c [9].

$$\tau = \frac{1}{2\pi(f_c/3)} \tag{2.4}$$

Vibration tests were made for MBT to determine the critical frequencies. For the MBT the tests are made in a project in ASELSAN. Barrel's natural frequency is determined in these tests as 10.73 Hz [10].

2.2.3 Dither Signal

Behavior of a hydraulic servo valve can be unpredictable because of stiction which keeps the valve spool from moving when input signal changes are small. When the signal finally becomes large enough to initiate a movement, the spool will tend to overshoot the position required for accurate control. Dither is a rapid, small movement of the spool around the desired position. It is intended to keep the spool moving to avoid stiction. Dither amplitude must be large enough and the frequency slow enough for the spool to respond, and yet small and fast enough to avoid creating a noticeable pulsation in the hydraulic output of the valve. The amplitude of the ripples determines whether, or how far, the spool will move at a given frequency [11,12].

The dither signal can be applied to the system by adding this signal to the control command. It is usually about 25-300 Hz and magnitude is the 10 % of the reference control signal. In addition to this property, the dither signal prevents the contamination near the orifices inlets which work very little openings [13]. Command signal used in the system is 10 V for the full opening of the servo valve. The 10 % of this value corresponds to the peak-to-peak value of the amplitude of the dither signal. Dither signal used in this

model is a sine wave with an amplitude 0.5 V at 140 Hz. These parameters are found in [7] and give the best performance without oscillation.

2.3. Actuator Model

Hydraulic actuator used in the system in this study is a double acting type as shown in Figure 15. The flow from the valve fills the actuator and pressurizes one side of the cylinder. Force required for the motion is produced by this pressurized liquid acting on the piston.

Actuator motion, fluid compressibility, actuator stiffness and the leakage in the actuator define the flow rate directly.

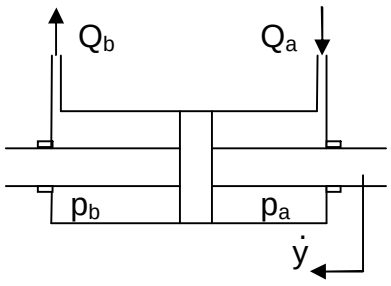

Figure 15. Double Acting Type Actuator

Finally the assumptions made while modeling the actuator is as follows.

- Temperature change in the fluid is neglected.
- Cylinder and pressurized lines are absolutely rigid.
- Piston mass is negligible.(Because barrel mass is too large)
- There is no internal leakage in the actuator.
- Compressibility is taken into consideration while volumes in the cylinder and its lines are too big compare to the servo valve.

Bulk modulus, β_e, is the measure of the compressibility of a fluid, defined as;

$$\beta_e = -V\frac{dp}{dV} \tag{2.5}$$

representing the stiffness of a hydraulic system. As the bulk modulus becomes bigger, the fluid becomes stiffer.

The compressibility is taken into consideration only while modeling the actuator because volumes in the actuator and pressurized lines are too large than the volumes in the servo valve.

While it is assumed that leakage flow is zero and the cylinder is absolutely rigid, equation for the conservation of mass can be written as in the following form for the chambers (2.6a and b) [14].

$$Q_a = A_a\dot{y} + \frac{v_a}{\beta_e}\dot{p}_a \tag{2.6a}$$

$$Q_b = A_b\dot{y} - \frac{v_b}{\beta_e}\dot{p}_b \tag{2.6b}$$

where;

Q_a : Flow rate into the cylinder's chamber a

Q_b : Flow rate out of the cylinder's chamber b

A_a, A_b : Net piston areas (rod area subtracted)

v_a v_b : Volumes of cylinder chambers

$\dot{p}_a$ $\dot{p}_b$: Time rates of changes in pressure in cylinder chambers

The causality relation between the flow rate, velocity of piston and the pressure can be explained as in Figure 16.

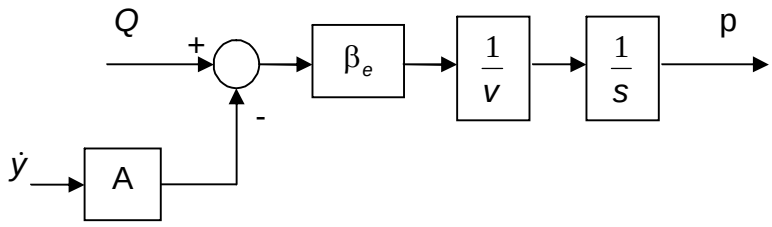

Figure 16. Causality Block Diagram of Flow Rate and Pressure

The net force produced in an actuator is the difference of the pressure forces at two sides of the piston.

$$F = p_a A_a - p_b A_b \tag{2.7}$$

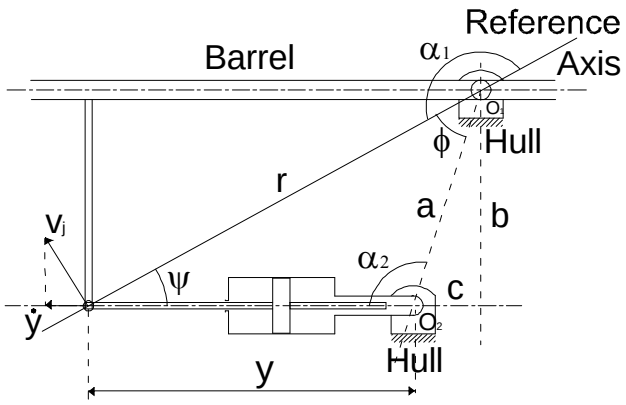

Figure 17. Barrel and Actuation (Slider Crank) Mechanism

The actuating system is a slider-crank mechanism in the system. The cylinder is fixed to the hull and the piston is mounted to the barrel like in Figure 17.

The output of the system is the barrel's angular position; input is the desired angular position of the barrel relative to the hull. On the other hand slider-crank has a translational input and a rotational output.

The unknown parameter which is the variable edge of the triangle for this mechanism is the length of the actuator. The loop closure equations are;

$$y\cos\alpha_2 = r\cos\alpha_1 + a \tag{2.8}$$

$$y\sin\alpha_2 = r\sin\alpha_1 \tag{2.9}$$

Solving the equations for α_1 and α_2;

$$\alpha_1 = \cos^{-1}\left(\frac{y^2 - r^2 - a^2}{2ar}\right) \tag{2.10}$$

$$\alpha_2 = \cos^{-1}\left(\frac{y^2 + a^2 - r^2}{2ay}\right) \tag{2.11}$$

Substituting (2.10) and (2.11) in definition of $\psi = \alpha_1 - \alpha_2$;

$$\psi = \cos^{-1}\left(\frac{y^2 - a^2 - r^2}{2ay}\right) - \cos^{-1}\left(\frac{y^2 + a^2 - r^2}{2ay}\right) \tag{2.12}$$

where;

y	:	Total length of piston and the cylinder
r	:	Radius of the rotation of barrel around the mounting to the hull
a	:	Length of the line connecting the mountings of the barrel and the cylinder to the hull
α_1	:	Angle between the reference axis and the r
α_2	:	Angle between the reference axis and the y
ψ	:	Angle between y and r

The relation between the rotational and the translational movement can be shown as follows.

$$V_j = \omega r \tag{2.13}$$

$$\dot{y} = V_j \sin\psi \tag{2.14}$$

where;

V_j : Tangential velocity of the piston about the instantaneous center of rotation

ω : Angular velocity of the barrel

r : Radius of the instantaneous center of rotation

Combining these two equations, gives

$$\dot{y} = \omega r \sin\psi \tag{2.15}$$

2.4. Barrel Model

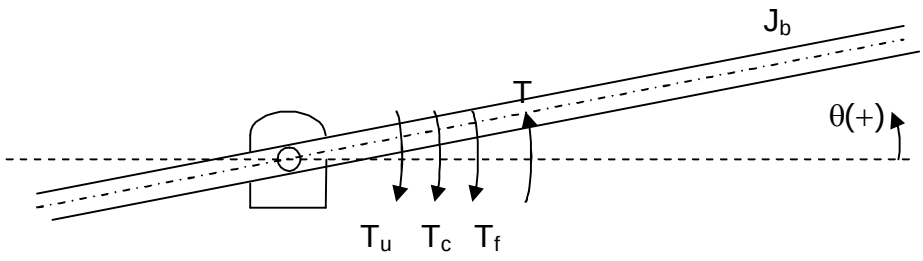

Figure 18. Torques acting on the Barrel

Referring to Figure 18 the equation of motion can be written as for the barrel.

$$J_b\ddot{\theta} = T - T_f - T_u - T_c \qquad (2.16)$$

where;

T	:	Torque applied to the barrel by the actuator
J_b	:	Mass moment of inertia of barrel
θ	:	Angular position of barrel
T_f	:	Viscous friction torque
T_c	:	Static friction torque
T_u	:	Unbalance torque

There are two hard-stops which limit the rotation of the barrel with respect to the hull at $+20^o$ and -10^o. Hence these limits are relative to the hull. Also the joint between the barrel and the hull is not located at the center of gravity of the barrel and has both Coulomb and viscous friction. Geometrical structure of the actuation system, frictions and unbalance cause nonlinearity. In addition to the general assumptions, the barrel is assumed to be absolutely rigid.

A classical *"Coulomb + viscous friction"* characteristic can be shown as seen in Figure 19 [15].

While modeling, causality must be carefully followed. To be able to start the motion, static friction, T_c, must be overcame. Thus, in determining the situation whether *"stick"* or *"move"*, coulomb friction will be the first check point.

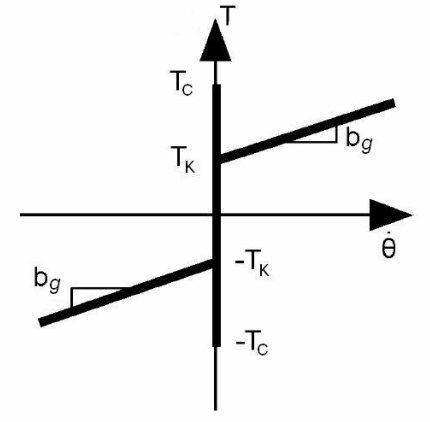

Figure 19. Coulomb + Viscous Friction Characteristics

The system is assumed to be stuck to the hull as the initial condition. Then the relative velocity will be zero and so will be the viscous friction. T_c^*, is the *"resultant torque"* of the actuation torque, unbalance torque and inertial torque. The resultant torque which tries to overcome the static friction torque can be defined as;

$$T_c^* = T - T_u - J_b\ddot{\theta}_T \tag{2.17}$$

where;

$\ddot{\theta}_T$: Angular acceleration of the turret

T_c^* : Resultant torque

Then, it is compared to the static friction torque. The barrel's status is defined with this comparison. The two possible results of this comparison can be shown as follows.

$$T_c \geq T_c^* \tag{2.18}$$

$$T_c < T_c^* \tag{2.19}$$

If the static friction is bigger than the resultant torque applied to the system, then the barrel will be stuck, otherwise barrel will move.

The other design criterion is the rotation limits of the barrel. It should not be forgotten that these limits are relative to the hull.

$$-10^{o} < \theta_R < +20^{o} \qquad (2.20)$$

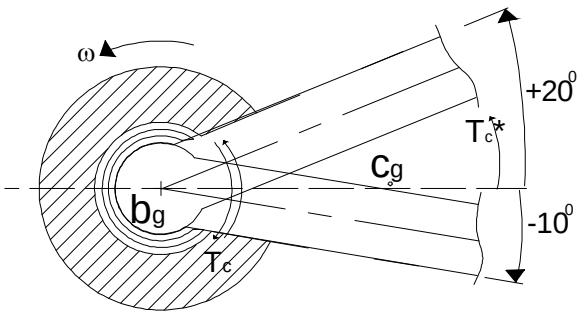

Figure 20. Simplified View of the Barrel Joint

A simplified projection of the joint which mounts the barrel to the gun could help the problem to be understood better (Figure 20). In this case, outer part has an angular velocity and it is known. There is viscous friction, represented by b_g, and static friction, T_c between the outer and the inner part. Resultant torque, T_c^*, was defined before.

These comparisons are illustrated in the flow diagram in Figure 21.

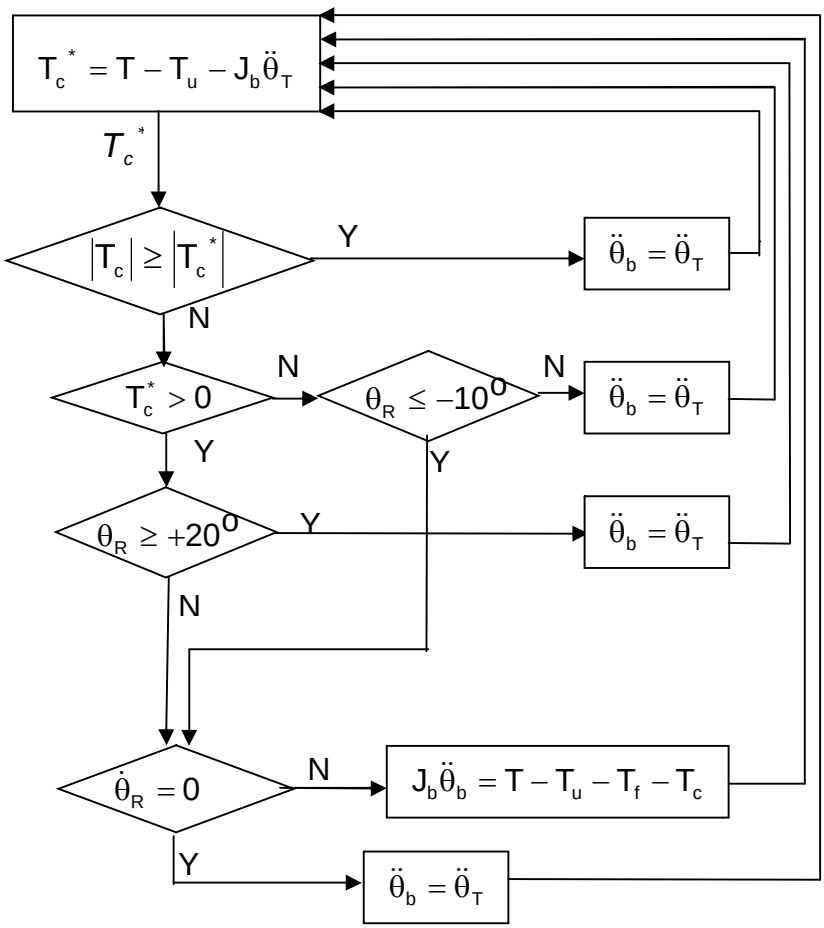

Figure 21. Flow Chart of Barrel Movement According to the Friction

Comparison of the friction torque and the resultant torque is made before to decide whether the motion starts or not. Since there are hard-stops, new comparisons should be made on the situation where the barrel is at limits in position.

While the barrel is at the negative limit, a resultant torque which is in the negative direction and naturally larger than the friction torque make no sense for the system. This torque tries to move the barrel beyond the limit and barrel is stuck in this situation. If the resultant torque is in the positive direction, barrel can move. On the other hand, when the barrel is at the positive limit, the direction effects on the system of the resultant torque are

just the opposite of the first two cases. These are the conditions of passing from stuck to slip.

Another decision should be made about whether the barrel continues its motion or stops. Relative velocity and the position of the barrel are criteria for this case. Barrel sticks to the hull when any of the two conditions are satisfied. These two conditions are considered at the same time. One is the position check of the barrel whether it touches the hard-stops or not and the other is the velocity comparison of the inner part with the outer one.

2.4.1. Unbalance Effect

The unbalance is the result of the mounting the barrel to the hull from any where except its center of mass. Its effect on the barrel is an additional torque proportional to the displacement between the center of mass and the mounting and the angular position of the barrel with respect to the hull. The hull is assumed always parallel to the ground (Figure 22).

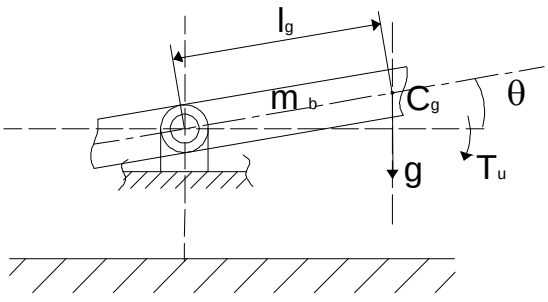

Figure 22. Unbalance Effect on the Barrel

The torque caused by the unbalance effect can be determined as follows.

$$T_u = m_b g l_g \cos\theta \qquad (2.21)$$

where;

T_u : Unbalance torque

m_b : Mass of the barrel

l_g : Distance between the center of rotation and center of gravity

However, this is not the only factor which cause torque on the barrel in vertical axis. While the tank moves on a curved surface, it rotates around an instantaneous center of rotation of ground profile (Figure 23). This affects the barrel as disturbance which is an angular velocity. The rate of change of the angular velocity, α_d is the acceleration and causes torque in the system in the opposite direction with the angular velocity.

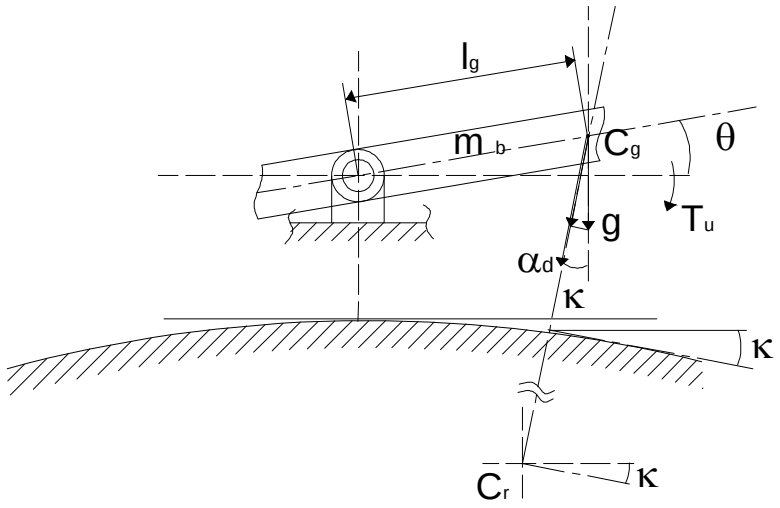

Figure 23. Instantaneous Center of Rotation and Normal Acceleration

By the addition of the normal acceleration to the system, the new unbalance torque equation can be rewritten as follows.

$$T_u = m_b(\alpha_d + g\cos\kappa)l_g\cos\theta \qquad (2.22)$$

where;

α_d : Normal acceleration

κ : Angle between the tangent of the surface and the normal of the rotation axis

As mentioned before, road profile affects the barrel as the disturbance which is an angular velocity. The rotation is unique all over the tank around the instantaneous center rotation.

While the tank moves on a curve, S, with a constant speed of v, it goes Δs much in Δt time. While this motion, vertical displacement of the barrel is Δy much.

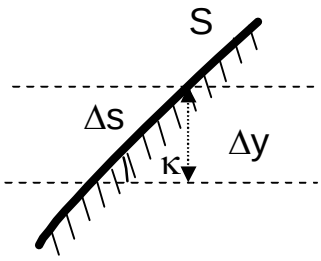

Figure 24. Angular Displacement on Road Profile

Angular displacement of the barrel is κ angle and angular velocity, demonstrated by ω, will be the change in κ angle. In this point of view, angular velocity, ω can be determined as follows.

$$\omega_d = \frac{d}{dt}\kappa \tag{2.23}$$

$$\Delta s = v\Delta t \tag{2.24}$$

$$\sin\kappa = \frac{\Delta y}{\Delta s} \tag{2.25}$$

Substituting (2.24) in (2.25) and (2.26) will give

$$\sin\kappa = \frac{\dot{y}}{v} \tag{2.26}$$

$$\kappa = \sin^{-1}\left(\frac{\dot{y}}{v}\right) \tag{2.27}$$

And from the definition of the angular velocity, it can be determined as

$$\omega_d = \frac{d}{dt}\left[\sin^{-1}\left(\frac{\dot{y}}{v}\right)\right] \tag{2.28}$$

Hence, the disturbance affecting on the barrel caused by the road profile is found.

CHAPTER 3

CONTROL STRATEGIES FOR DISTURBANCE REJECTION

Although different systems are designed to perform different functions, all of them have to meet some common requirements. Main characteristics of a typical system concern accuracy, speed of response and output sensitivity to component and environmental changes. The priority of importance of these characteristics is defined by the designer based on the system nature and its application. These characteristics are used to measure the performance of the system. But the primary concern is the stability of the system.

In this study, all of the criteria were tried to be satisfied but according to this specific application most important performance criteria is disturbance rejection in other words stabilization of the barrel in the elevation axis when the MBT moves on a bumpy road.

3.1. Controller

System has two outputs to be controlled namely the angular velocity and the position. Each loop, which are constructed by feeding back the system output to the comparison with the desired value, is controlled by a PID controller. The position and the velocities in the system are measured by different devices. The device used for measuring the velocity is a classical mechanical gyroscope both for the barrel and the hull. The position of the barrel is measured by an inclinometer. At first look, it seems meaningless but the feedback signals are supplied from different sources. The gyroscopes used in the system have a bandwidth of 30 Hz and a damping ratio

of 0.7. Although they are relevant, in industrial applications controllers could be used in this way.

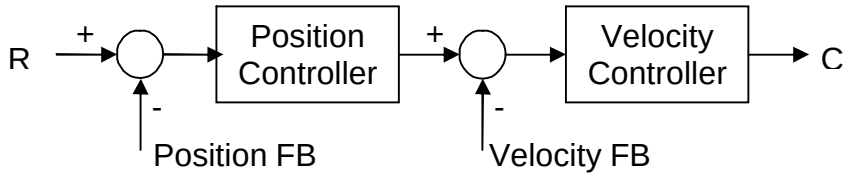

Figure 25. Classical Control Algorithm

Many parameters in the system and environment try to determine or affect the system output. System characteristics itself, while it has many nonlinearities, disturbances influence the controllers efficiency. Thus, some additional strategies may be used to eliminate these effects on the system to reject the disturbances more effectively.

3.2. Disturbance Feed Forward

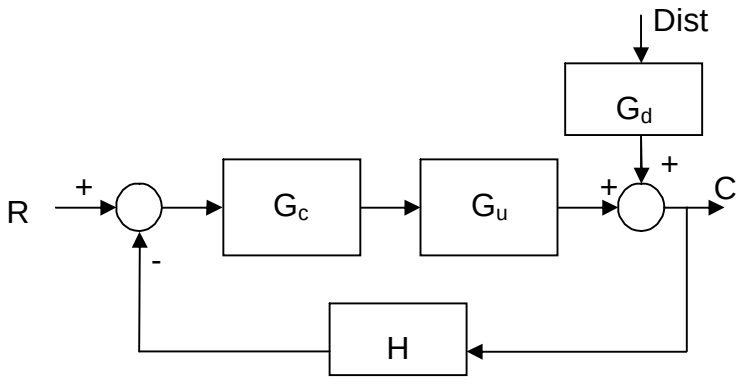

Figure 26. Feedback System with Disturbance Input

As the definition of disturbance, it is unwanted that adversely affect the desired output (Figure 26). Although the effect of disturbances on the system can not be eliminated completely, it can be reduced. To be able to improve the response, first of all disturbance must be determined [16].

To nullify the disturbance effects on the system, disturbance can be fed back to the input of the plant as seen in Figure 27.

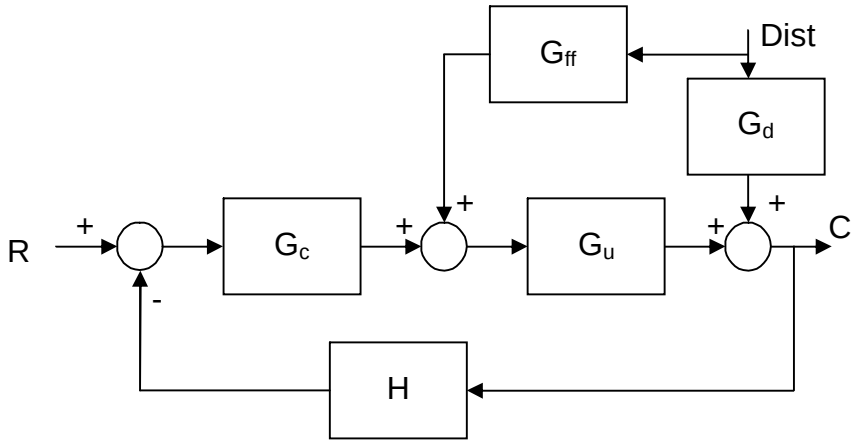

Figure 27. Feedback System with Disturbance Feed Forward

Ideally, the feed forward transfer function, G_{ff}, should be the inversion of the ratio of the disturbance transfer function and the nominal plant transfer function. It is not forgotten that the G_{ff} must be stable since it acts in open loop [17].

$$G_{ff} = -\frac{G_d}{G_u} \qquad (3.1)$$

Frequency response of the system is analyzed to be able define the transfer function, G_u, between the command signal and the output.

Table 1 Frequency Response Data for G_d and G_u.

	Gd			Gu		
Frequency (Hz)	**20log M (dB)**	**Mag of input**	**Mag of output**	**20log M (dB)**	**Mag of input**	**Mag of output**
0.1	0.0054	0.2	0.2001	0.1998	0.2	0.1996
0.2	0.0506	0.2	0.2012	0.539	0.2	0.2128
0.3	0.055	0.2	0.2013	0.6656	0.2	0.2159
0.4	0.0796	0.2	0.2018	0.7432	0.2	0.2179
0.5	0.0867	0.2	0.202	0.8005	0.2	0.2193
0.6	0.0962	0.2	0.2022	0.8483	0.2	0.2205
0.7	0.1115	0.2	0.2026	0.8915	0.2	0.2216
0.8	0.1239	0.2	0.2029	0.9324	0.2	0.2227
0.9	0.1506	0.2	0.2035	0.9742	0.2	0.2237
1	0.1407	0.2	0.2033	1.016	0.2	0.2248
2	0.1729	0.2	0.204	1.5484	0.2	0.239
3	0.3445	0.2	0.2081	2.342	0.2	0.2619
4	0.5439	0.2	0.2129	3.3323	0.2	0.2935
5	0.6408	0.2	0.2153	4.4074	0.2	0.3322
6	0.9606	0.2	0.2234	5.2972	0.2	0.368
7	1.0884	0.2	0.2267	5.5959	0.2	0.3809
8	1.4413	0.2	0.2361	5.1497	0.2	0.3618
9	1.6767	0.2	0.2426	4.1001	0.2	0.3207
10	1.7434	0.2	0.2445	2.7229	0.2	0.2736
13	2.0475	0.2	0.2532	0.4917	0.2	0.2116
16	3.1989	0.2	0.2891	-1.0748	0.2	0.1767
20	7.1993	0.2	0.4581	-2.0245	0.2	0.1584
23	8.5271	0.2	0.5338	-0.9974	0.2	0.1783
26	13.6972	0.2	0.968	0.3915	0.2	0.2092
30	25.8101	0.2	3.9042	-0.1859	0.2	0.1958
33	11.3783	0.2	0.7412	-3.1657	0.2	0.1389
36	5.7344	0.2	0.387	-8.6341	0.2	0.074
40	4.6665	0.2	0.3422	-14.1794	0.2	0.0391
50	-2.0602	0.2	0.1578	-23.9876	0.2	0.0126
60	-5.9759	0.2	0.1005	-30.9814	0.2	0.0056
70	-8.6592	0.2	0.0738	-36.5776	0.2	0.003
80	-10.7546	0.2	0.058	-41.0167	0.2	0.0018
90	-12.6257	0.2	0.0467	-44.7575	0.2	0.0012
100	-14.0877	0.2	0.0395	-47.6867	0.2	0.0008

Identification of the disturbance transfer function, G_d, and the transfer function of the nominal plant are made by using the frequency response. This identification is made on the Simulink® model.

In tests, system is separated from the controller and naturally from the loops. System is used as open loop. Only servo valve position feedback, LVDT is closed. Coulomb friction is neglected. Both input command to the open loop system and disturbance are sine wave at an amplitude of 0.1 rad/s with different frequencies.

Angular velocity demand which is fed to the system model at different frequencies with an amplitude of 0.1 rad/s is checked whether it cause any saturation in the system or not. After recording the outputs Bode plot can be obtained.

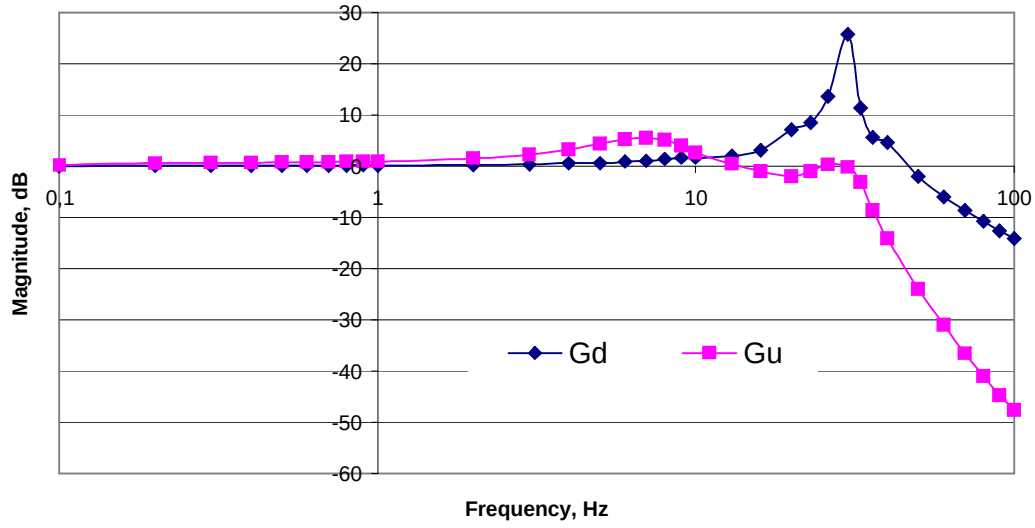

Figure 28. Bode Plot of Plant's and Disturbance Transfer Functions

As seen from the figure, transfer functions have a low pass characteristics and it should be expected that the G_{ff} must have a high pass characteristic. Corner frequency can be easily determined from Figure 28 as 27 Hz or approximately 170 rad/s.

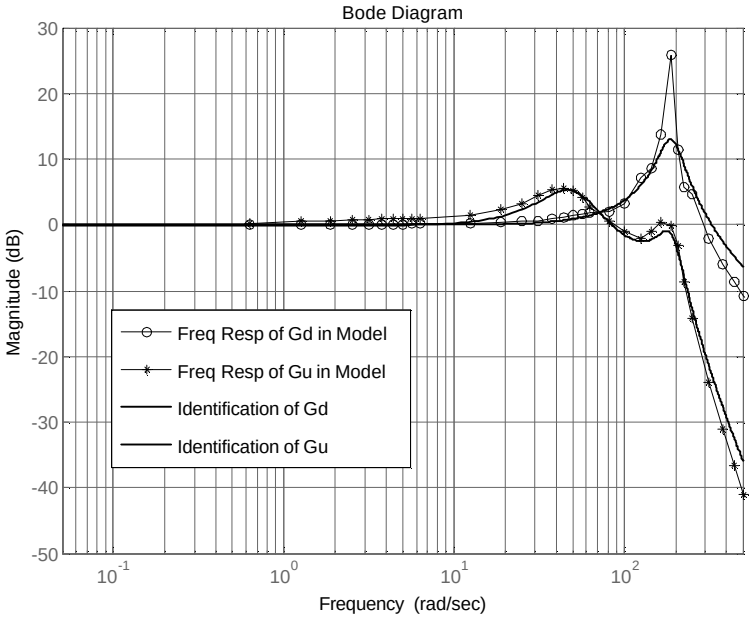

Figure 29. Bode Plot of the Disturbance and the Plant and the Identifications

At the end of the identification of G_d and G_u as seen in Figure 29, the transfer functions can be written as follows.

$$G_d = \frac{0.08469s^3 + 18.92s^2 + 796.8s + 36100}{0.0004s^4 + 0.04032s^3 + 16.41s^2 + 638.4s + 36100} \quad (3.2)$$

$$G_u = \frac{680s + 35360}{0.0004s^4 + 0.04032s^3 + 16.41s^2 + 638.4s + 36100} \quad (3.3)$$

To prevent the system from the disturbance, feed forward transfer function must be as follows.

$$G_{ff} = -\frac{0.08469s^3 + 18.92s^2 + 796.8 + 36100}{680s + 35360} \tag{3.4}$$

This is a high pass filter but it is impossible to realize that. Because this transfer function does not represent a physical system. Also the derivative terms will bring to the system more oscillations while disturbance itself is oscillatory. Instead of this, a realizable high pass filter can be used which is constructed adding poles which are very high frequency for the system as in Figure 30 [17]. Adding poles to the system at -700 will be adequate because the bandwidth of the elevation axis model is approximately 200 rad/s.

$$G_{ff} = -\frac{0.08469s^3 + 18.92s^2 + 796.8 + 36100}{0.001388s^3 + 2.015s^2 + 781s + 35360} \tag{3.5}$$

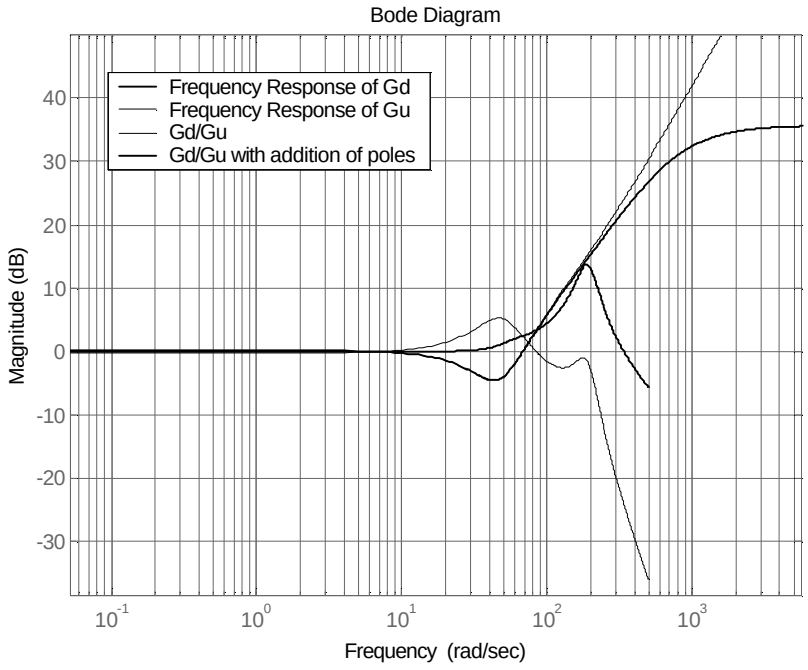

Figure 30. Bode Plot of the Disturbance Feed Forward Transfer Function

3.3. Feed Forward in Velocity Loops

Feed forward gains are used to speed up the response to rapidly changing position commands. Feed forward is often used in the cascaded position velocity loop. In this system, position loop enclose the velocity loop which is faster than itself. The feed forward path speeds response by-passing the slower position loop directly to the velocity loop (Figure 31).

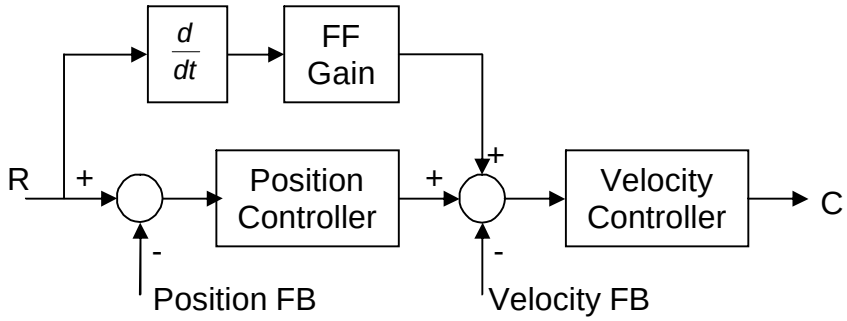

Figure 31. Velocity FF in Controller

In general, servo systems need high loop gains to have a good performance. High loop gain helps the controller to respond and reject disturbances. Since high servo gains may cause instability, they can be used limitedly. Thus feed forward can greatly improve the performance of a servo system.

The velocity feed forward path connects the velocity profile to the velocity loop through a gain. When the position profile abruptly changes, the velocity feed forward immediately passes that change to the velocity command. Velocity feed forward can reduce the time to make instant movement. But the disadvantage of this choice is produce overshoot. This can be settled by reducing the loop gains but to make this means also reduce the system disturbance rejection [18].

CHAPTER 4

SIMULATION

In this chapter, Simulink® models of the system components will be constructed and explained. Especially, servo valve identification and the friction model are handled in detail. Finally the complete system will be simulated for different cases. The simulations are made with a fixed time step of $5x10^{-4}$ s and the ODE5 (Dormand-Prince) solver is used. Because the fastest component of the system is the servo valve and its time constant is 0.0032 s. Since time step is very small, solution method also is selected 5^{th} order to be able to prevent the valuation error.

4.1. Valve Model and Identification Results

As explained in Chapter 2, the valve is separated into 2 parts. First part is made up of the linearized section which has the transfer function between the input voltage and the output valve's third stage spool position. Second part is the section where the flow is determined which maintains the nonlinearity of the orifices.

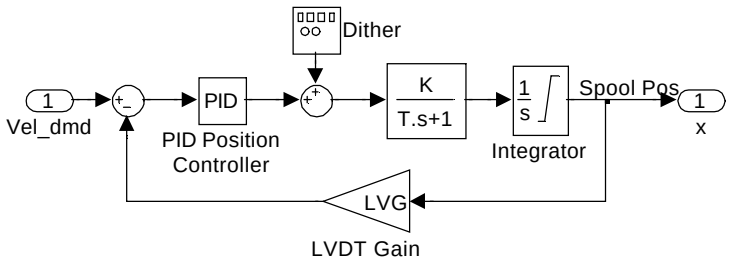

Figure 32. First Stage of the Servo Valve Model

In first stage as seen Figure 32, a dither signal is added to the input of the servo valve to be able prevent valve from hydraulic lock.

In the second part, nonlinear orifice equation is solved. By using (2.1) flow can be derived as;

$$Q_a = C_d w x_3 \sqrt{\frac{2}{\rho}(P_S - P_a)} \tag{4.1}$$

$$Q_b = C_d w x_3 \sqrt{\frac{2}{\rho}(P_b - P_e)} \tag{4.2}$$

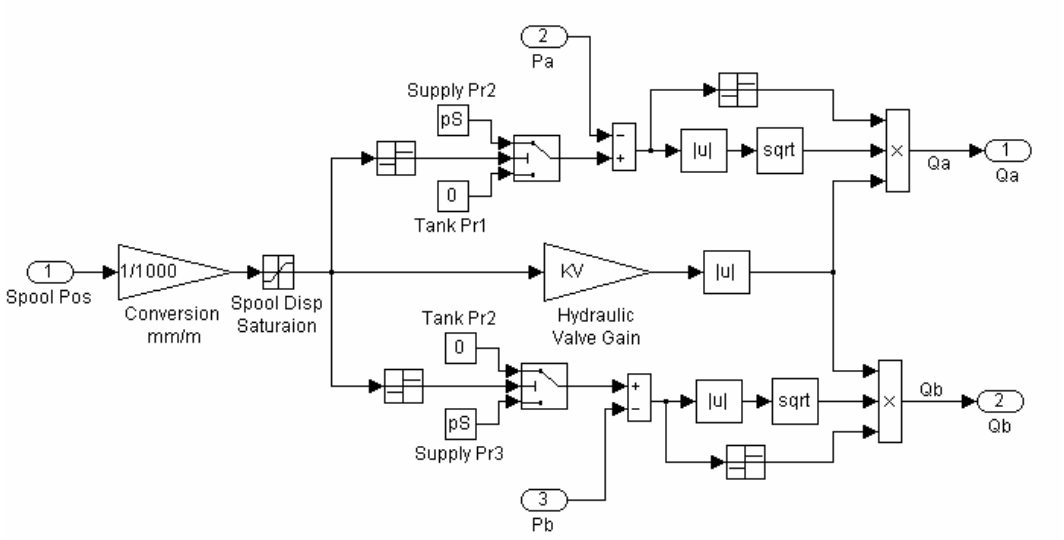

Figure 33. Flow Characteristics Model of the Servo Valve

The hydraulic conductance of an orifice can be shown as follows.

$$g_c = C_d w x \sqrt{\frac{2}{\rho}} \tag{4.3}$$

The only variable defining the conductance is the valve spool position, x_3. The others are constant terms and can be defined as follows for the simplicity of the model.

$$K_v = C_d w \sqrt{\frac{2}{\rho}} \tag{4.4}$$

By defining the other components as the *"Hydraulic Valve Gain"* flow rates can be rewritten as follows.

$$Q = K_v x_3 \sqrt{\Delta p} \tag{4.5}$$

By combining these two blocks complete servo valve block is constructed as seen in Figure 34. At this time, load pressure feedback is added to the valve. Load Pressure is fed back via a pressure transducer and high pass filter. High pass filter time constant is determined according to the load resonant frequency which is mentioned in Chapter 2 as $\tau = 0.445$ s. Scale for the input rad/s to mm is found by simulating the complete system with different inputs and take the ratios with the angular velocity output. Corresponding valve openings are determined and the scale is obtained.

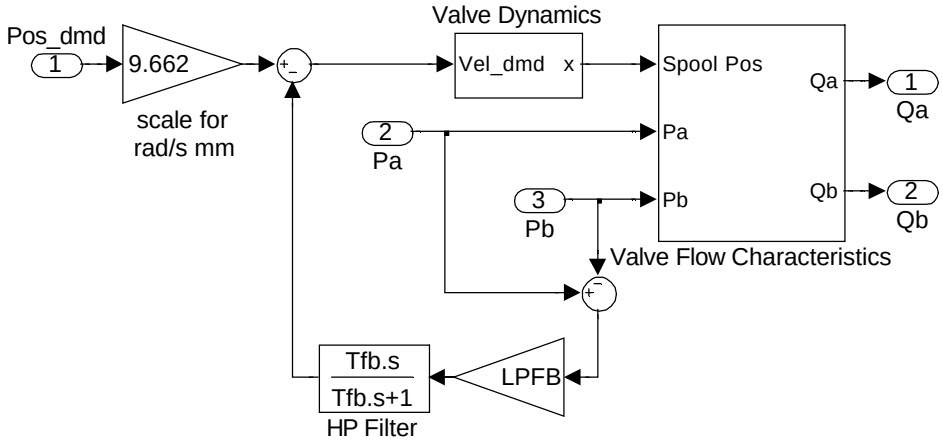

Figure 34. Servo Valve Model

4.1.1. Valve Identification

Servo valve is made up of three stages but there were the LVDT output and the command voltage as the input. The number of the step responses in Figure 14 was not equal for each amplitude. While the mean value will be determined, this inequality gives wrong weigh to the magnitudes. Identification is made by using the cost function via an “m” file which calculates the error between the simulation and the actual response by simulating the servo valve model with different gain and time constant parameters. In this calculation two actual step response data are used for each amplitude. Minimum error surface and the simulations with the parameters found in this case were plotted. The “m” file used for this identification can be found in Appendix 1.

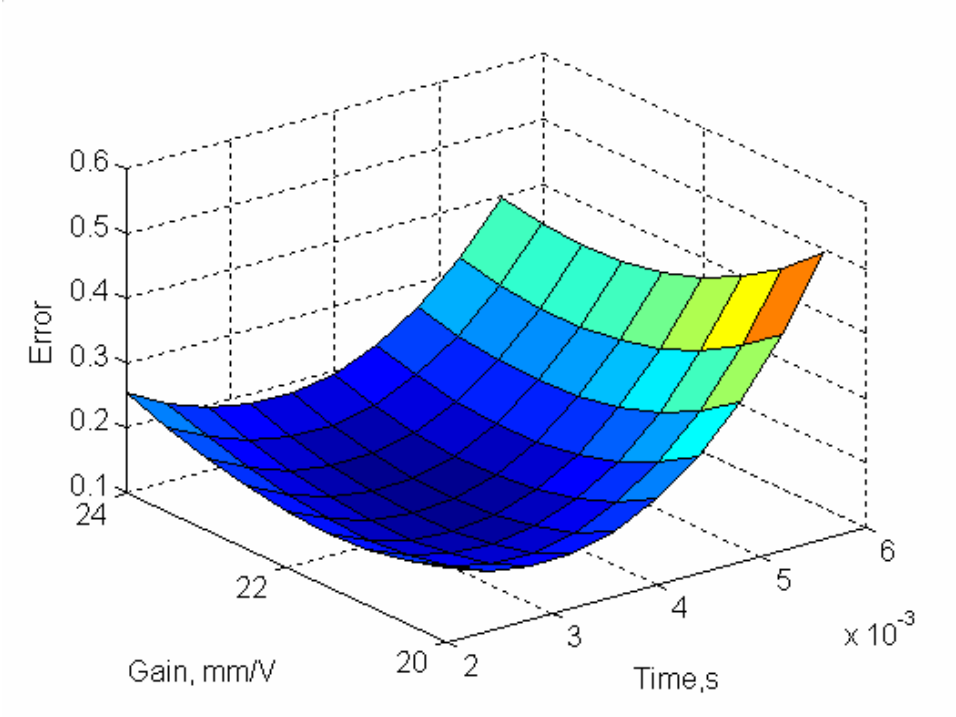

Figure 35. Error Surface for Servo Valve Identification

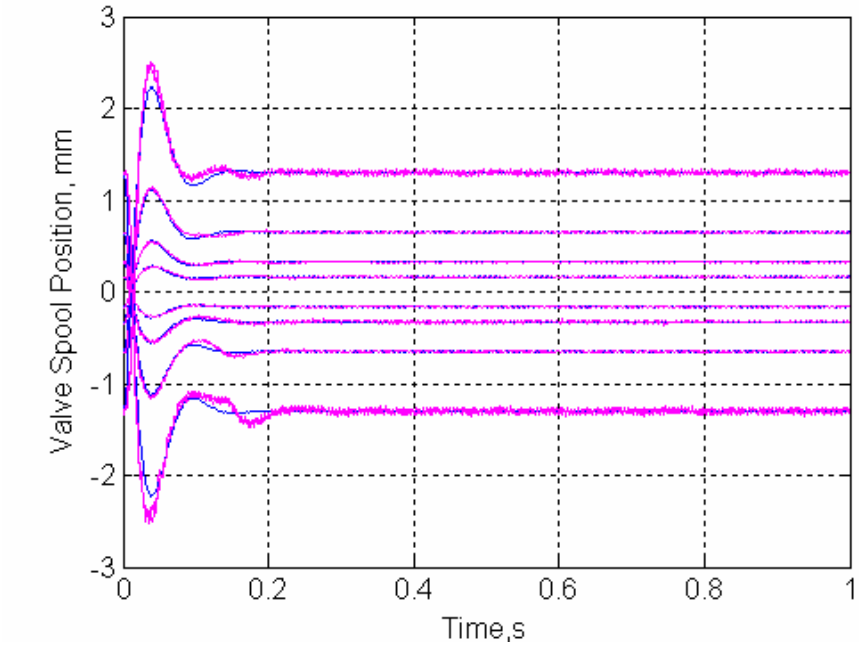

Figure 36. Servo Valve Simulation and Experiment Comparison

After these calculations, gain value, K, is found 21.8 and time constant , T, is found 0.0032 s.

4.2. Actuator Model

In actuator, there are two important components which must be considered. One of them is compressibility of the hydraulic fluid and the other is the inverse kinematics of the slider-crank mechanism i.e., determination of the piston position and velocity, as seen in Figure 37.

While finding the position of the actuator, initial condition is found by the position of the barrel. Also actuator stroke length is considered. Although the piston areas are equal, the model is designed to solve any actuator which has different areas. Finally it is assumed that the stroke will never touch the cylinder wall. So the corresponding dead volume in cylinder is considered in solution (Figure 38).

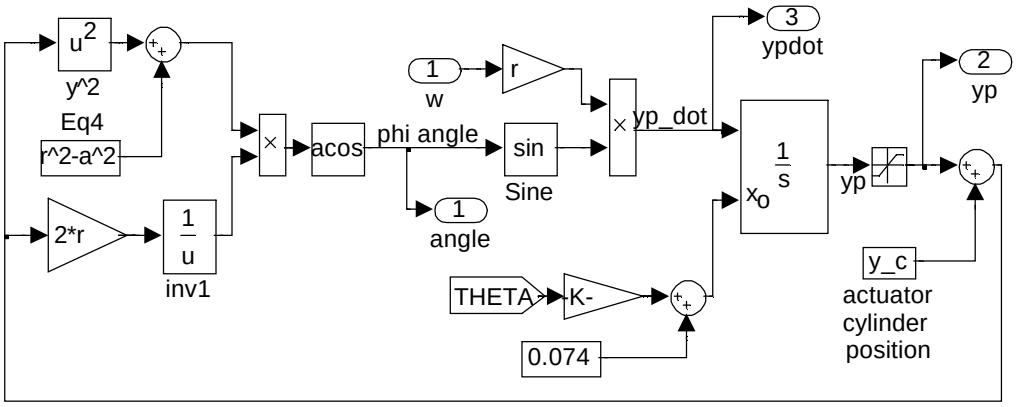

Figure 37. Inverse Kinematics of Slider-Crank Mechanism

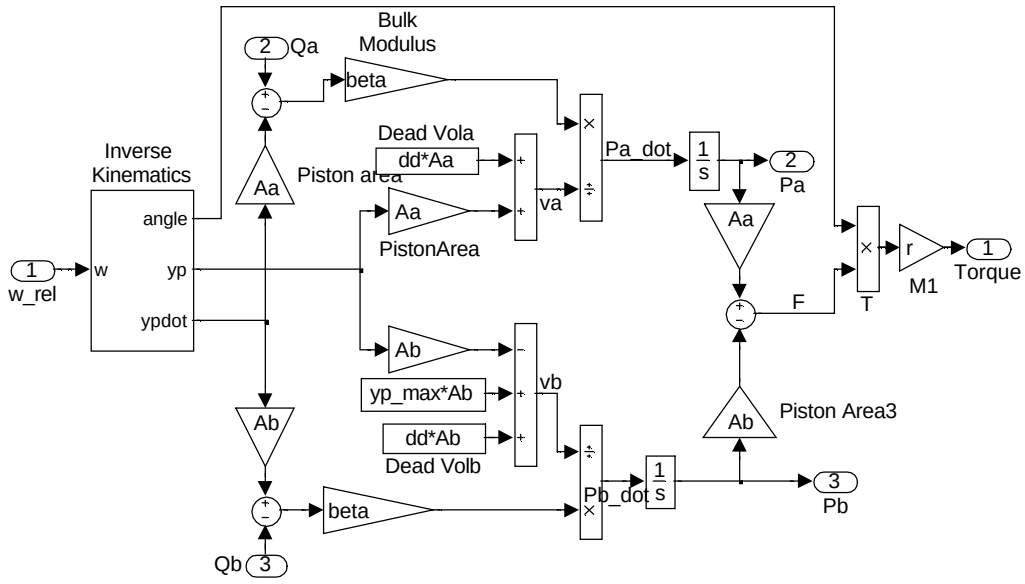

Figure 38. Actuator Model in Simulink

4.3. Friction Test Results

Friction model is considered to be done separately. The simplified barrel which is explained in Chapter 2 in Figure 20 is modeled. The frictions and the mechanical limits are considered. Unbalance effect is not included. In this example, parameters are not the same as the original system. These are just for the representation for different cases. Simulink® model can be seen in Figure 40.

In this model, friction characteristic which is defined in Figure 20 is used. To determine the acceleration of the barrel, the classical derivative block is not used. Instead of it, derivative is calculated by the help of the memory blocks in Simulink®. Also another problem is the determining the point of zero cross of the relative velocity of the barrel. While the solution is made with fixed time steps *"Zero Cross Detection"* block can not be used. To overcome this problem, next step in the relative velocity is calculated by adding the

increment found by the derivative of the relative velocity and the time step. The sign change is detected between the relative velocities at the present and the next time step.

At first simulations, only torque was applied to the system while the disturbance is zero. Then only disturbance was applied to the system. The disturbance is an angular velocity at the joint which mounts the barrel to the hull. A series of torques and disturbances are selected to simulate. These can be found in Appendix 2 with the other simulation results.

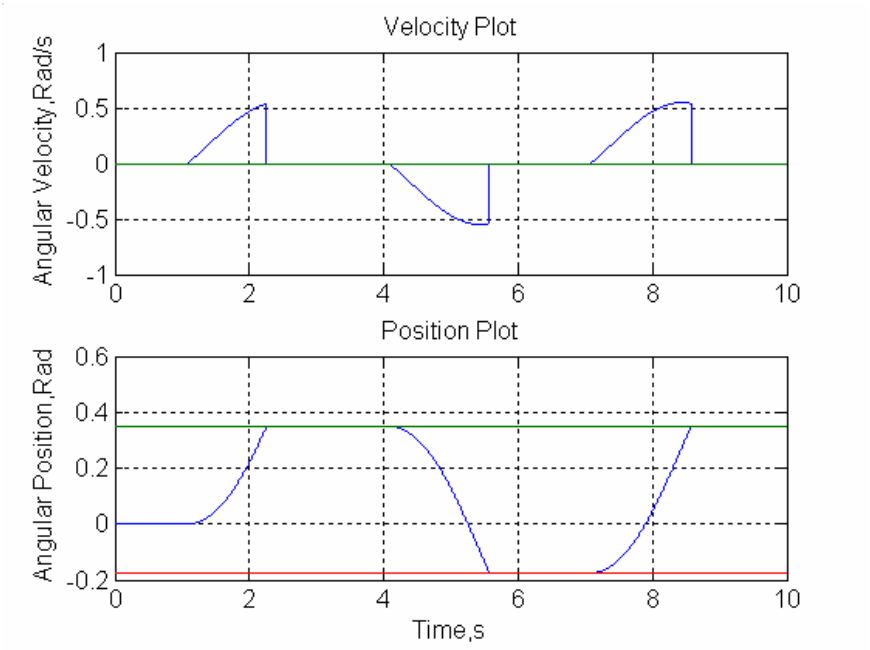

Figure 39. Velocity and the Position of Simplified Barrel

In Figure 39, there is no disturbance and the torque applied is sufficient to overcome the static friction. Hard-stops effects also can be seen.

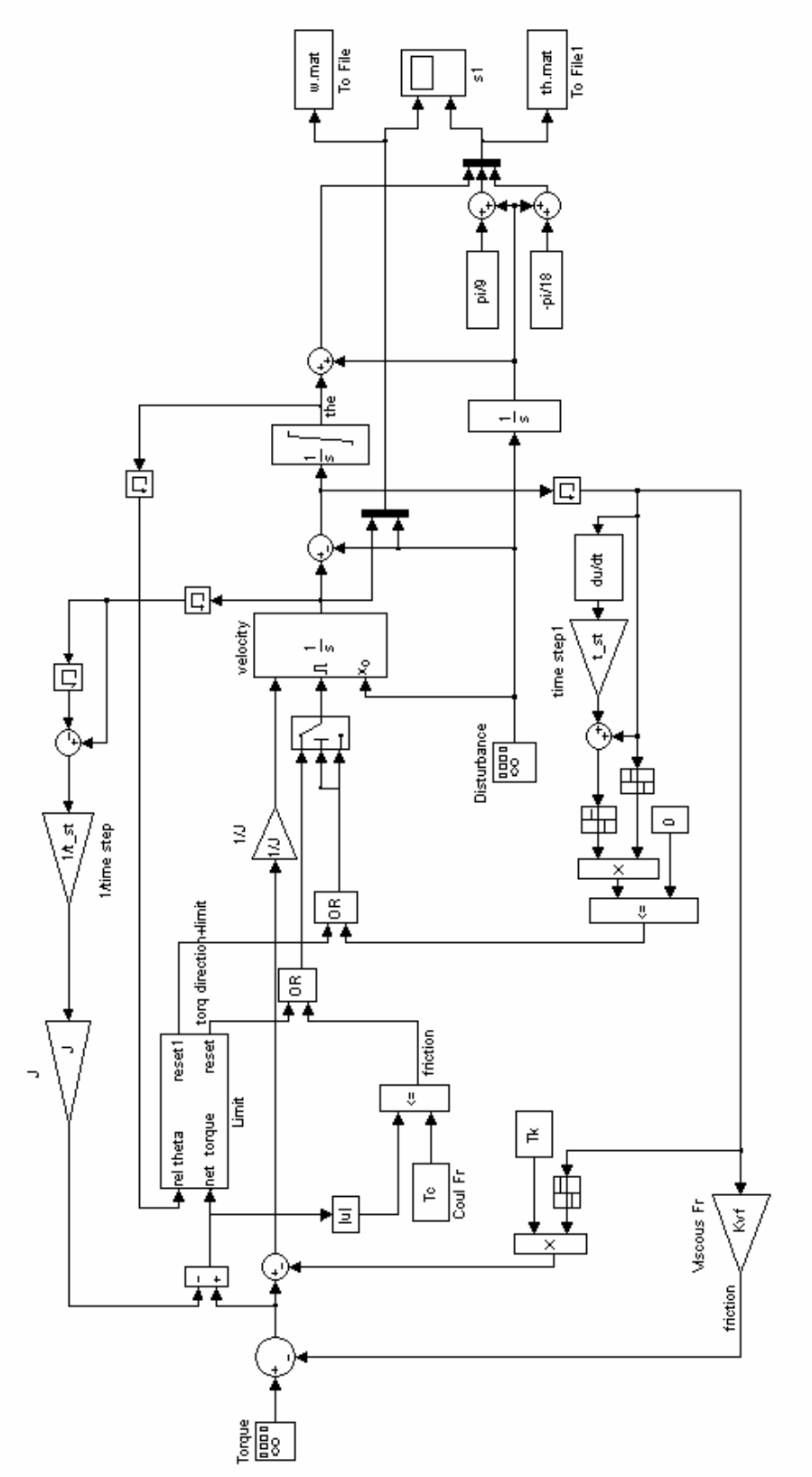

Figure 40. Friction Model

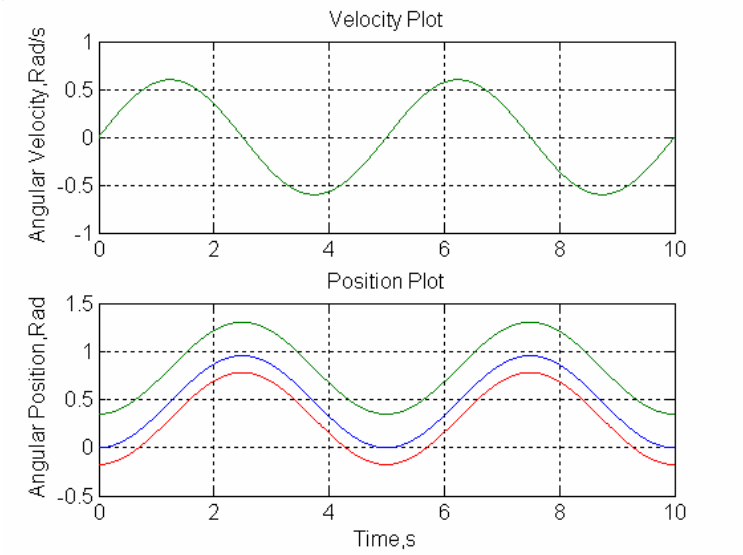

Figure 41. Velocity and the Position of Simplified Barrel

In Figure 41, only disturbance is applied to the system but the torque generated by disturbance is also not enough to move the barrel. Barrel velocity is at top of the hull velocity which is the disturbance.

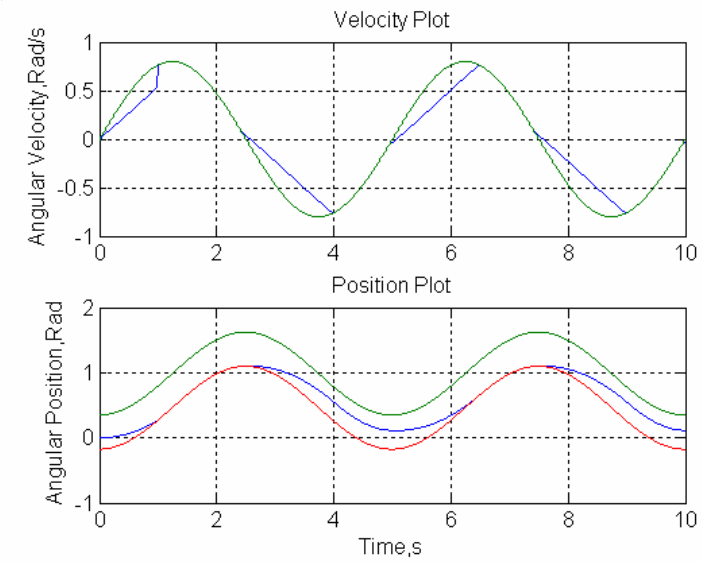

Figure 42. Velocity and the Position of Simplified Barrel

In Figure 42, disturbance is applied and friction is sometimes much more than the friction torque and caused the barrel rotates without touching the mechanical limits and be stuck when the friction decreases to a level less than the friction. In this situation velocity graphs have no jumps.

4.4. Barrel Model

The last component of the system is the barrel and it contains a logic block. This block checks the conditions which explained in Chapter 2 Section 4. According to the conditions, logic block decides whether the barrel moves or stops at the next time step and selects the corresponding friction torque to this motion. By controlling the relative velocity and the physical limits, it defines the stop conditions and resets the integral block after this decision.

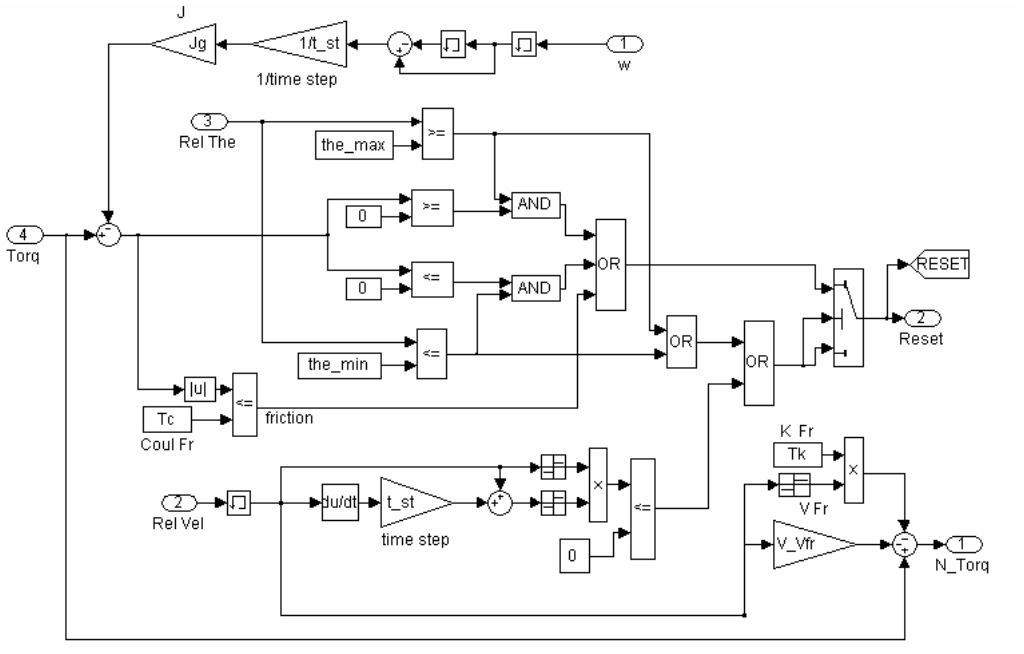

Figure 43. Friction and End-Stop Logic Block in Barrel Model

Inertial torque is taken into consideration. Disturbance originates from the road profile is also used in this part of the model. The mechanical limits which are relative to the hull are demonstrated by the limited integrals (Figure 43).

4.5. System Simulation

Controller of the system consists of two PIDs. Velocity and position of the barrel are fed back. Each loop is controlled by one PID controller. In addition to this, for disturbance rejection, disturbance is fed forward to the controller as seen in Figure 44.

Disturbance feed forward were examined in Chapter 3. Transfer Function of the disturbance feed forward is found from (3.5) as follows;

$$G_{ff} = \frac{0.08469s^3 + 18.92s^2 + 796.8 + 36100}{0.001388s^3 + 2.015s^2 + 781s + 35360} \qquad (4.6)$$

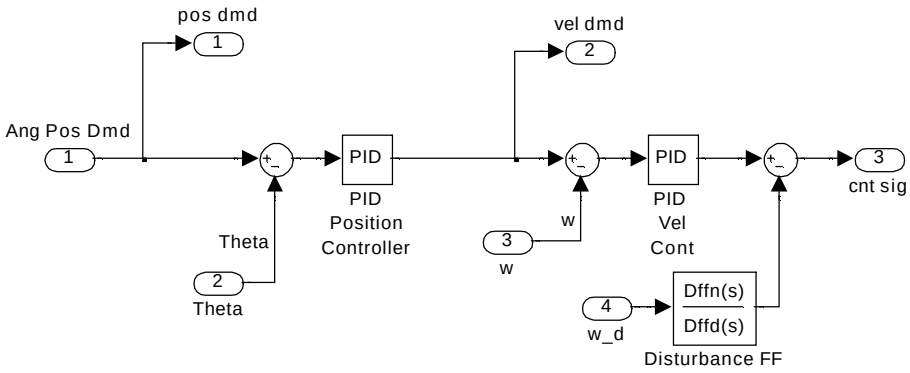

Figure 44. Controller of the System

The other choice to improve the controller is feeding forward the derivative of the position to the velocity controller. (Figure 45)

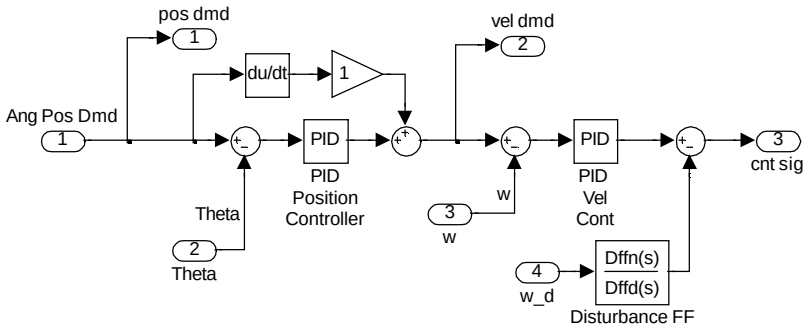

Figure 45. Controller of the System with Velocity FF

The complete barrel model will be as in Figure 46.

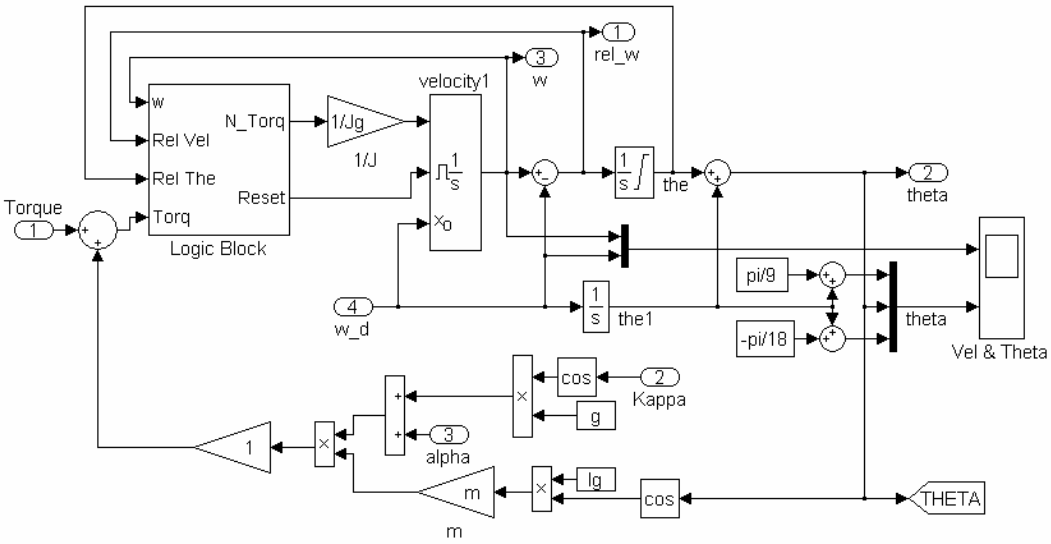

Figure 46. Barrel Dynamics Model

Controller parameters are tuned while a step command which does not cause the barrel hit to the hard-stops is applied to the system. Tuning process used in controller is as follows [19].

1. Set all gains zero.
2. Apply a step command.
3. Raise proportional gain until the system begins overshoot.
4. Raise integral gain until overshoot is approximately 15 %.
5. Raise derivative gain to remove some of the overshoot.

Step response of the barrel is shown in Figure 47.

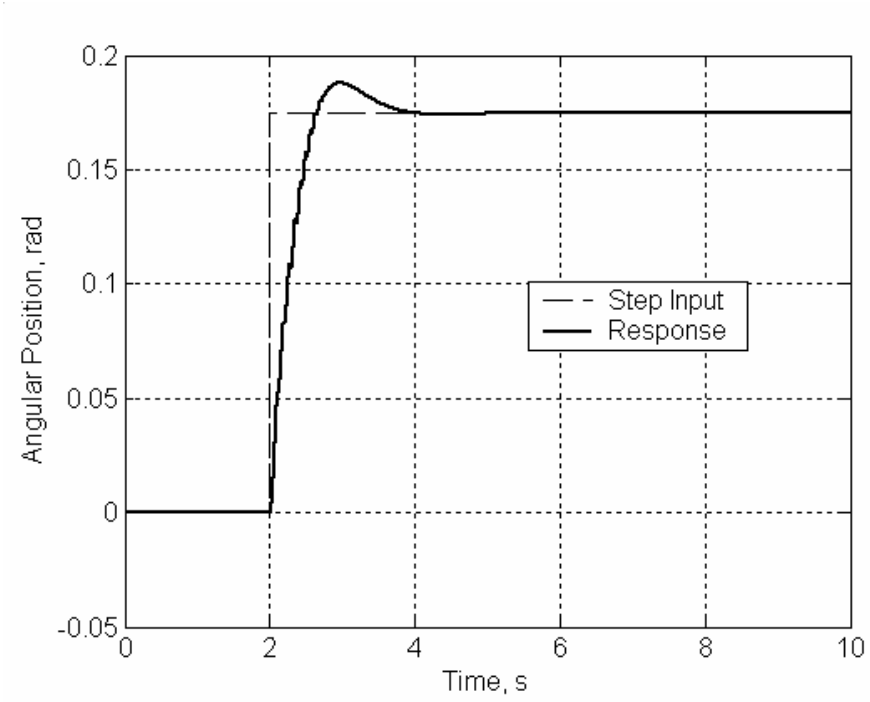

Figure 47. Step Response of the System

PI is used for the position control and PID is used for velocity control. Parameters of the PID controllers used in the simulations are shown in Table 2.

Table 2 PID Parameters used in the Simulations

Parameters	Position Controller	Velocity Controller
Kp	5	1.2
Ki	0	5
Kd	0	0

Control strategy mentioned before is used by adding velocity feed forward to the controller. System input is a sine wave which is saturated before the peaks. Hence, the error while taking the derivatives of the command signal is prevented. Also feed forward is scaled with a gain to tune the effect of the feed forward on the command signal. The outputs are plotted in Figure 48 and Figure 49.

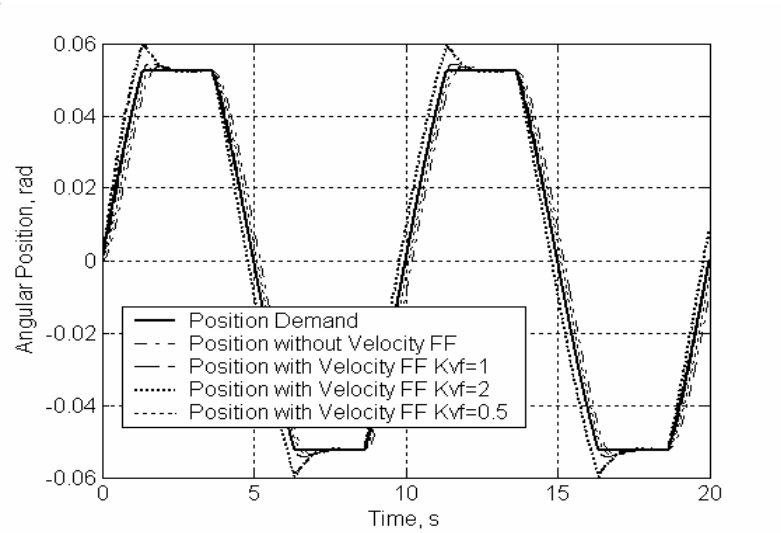

Figure 48. Comparison of the Responses for Different Velocity FF Gains

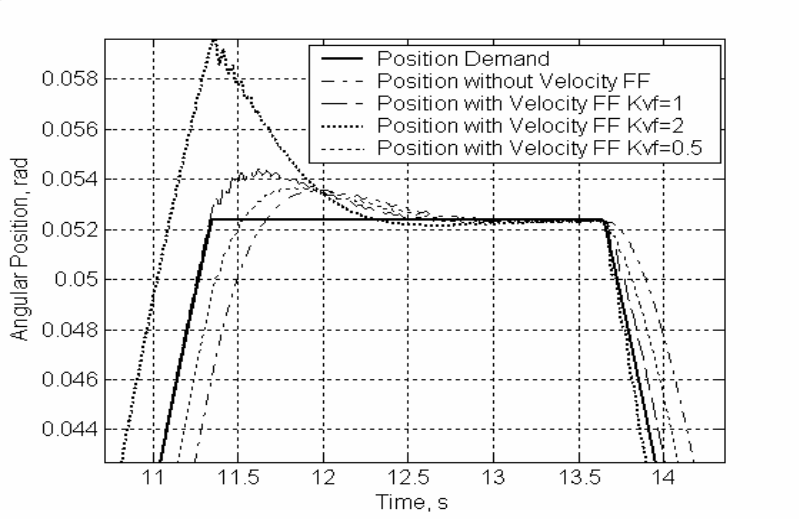

Figure 49. Zoomed View of Figure 48

According to the comparisons above, unity gain for the velocity feed forward should be used.

Two case studies are realized (Figure 50). In the case studies MBT is accepted to be moving with a fixed velocity of 20 km/h and 40 km/h. The road profile used in the simulation is a sine wave (Figure 51). Velocity feed forward is included in controller. The other system parameters can be found in Appendix 3.

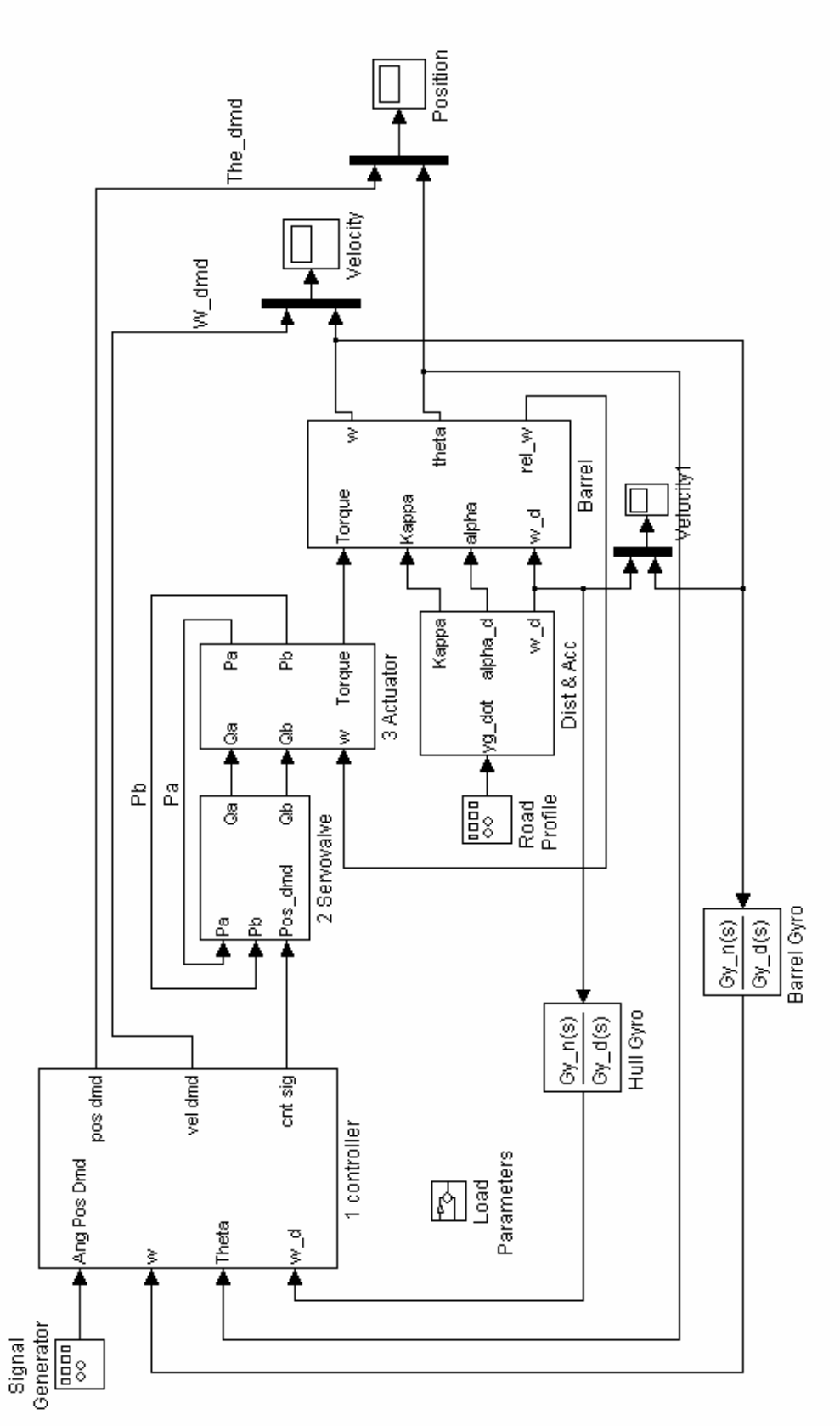

Figure 50. Barrel Stabilization System

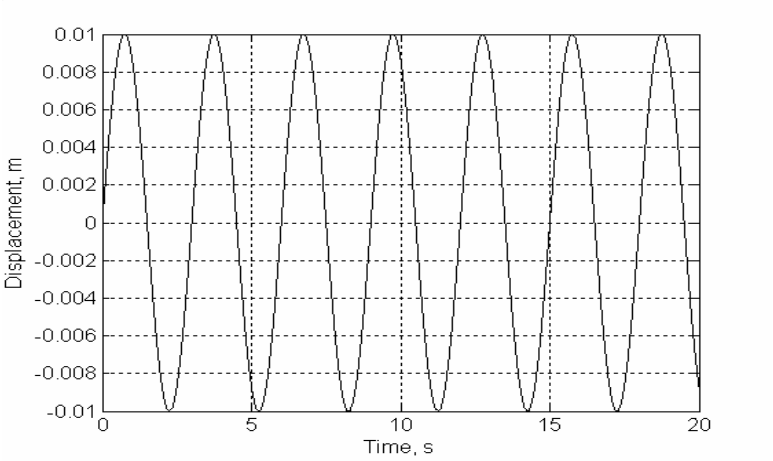

Figure 51. Road Profile

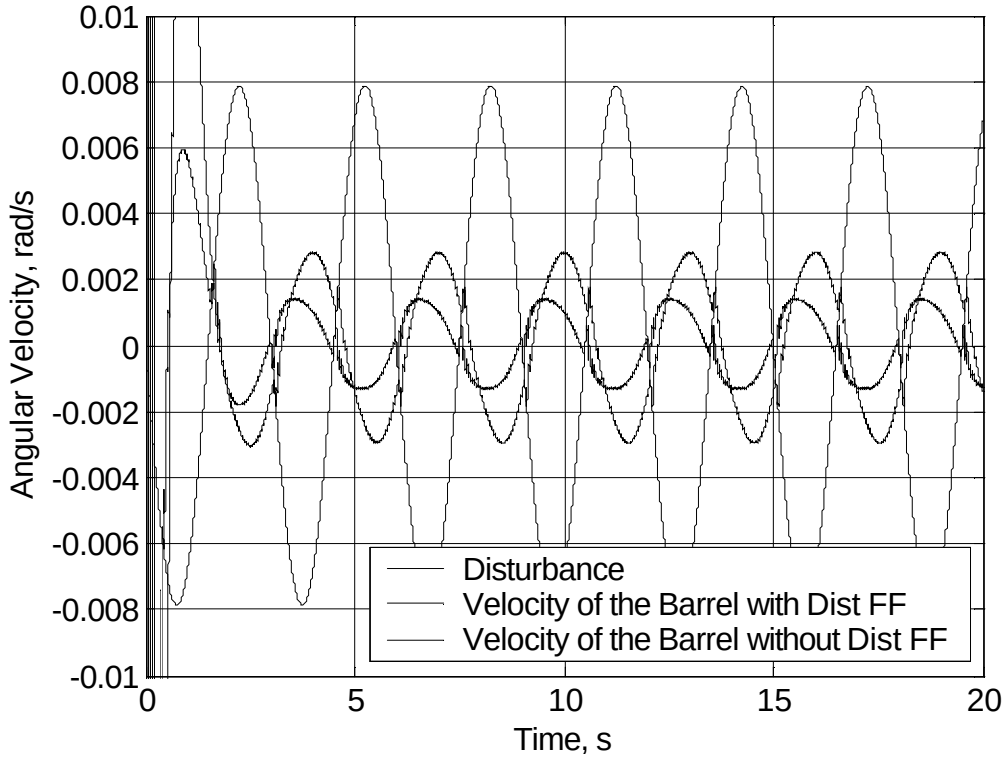

Figure 52. Disturbance and Effect Disturbance FF with a Velocity of V=20 km/h

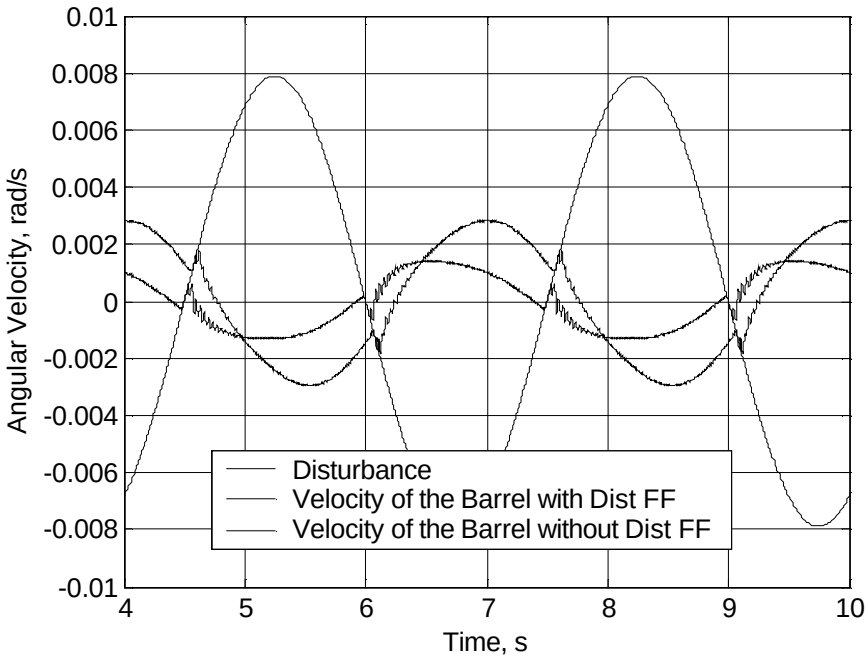

Figure 53. Zoomed View of Figure 52

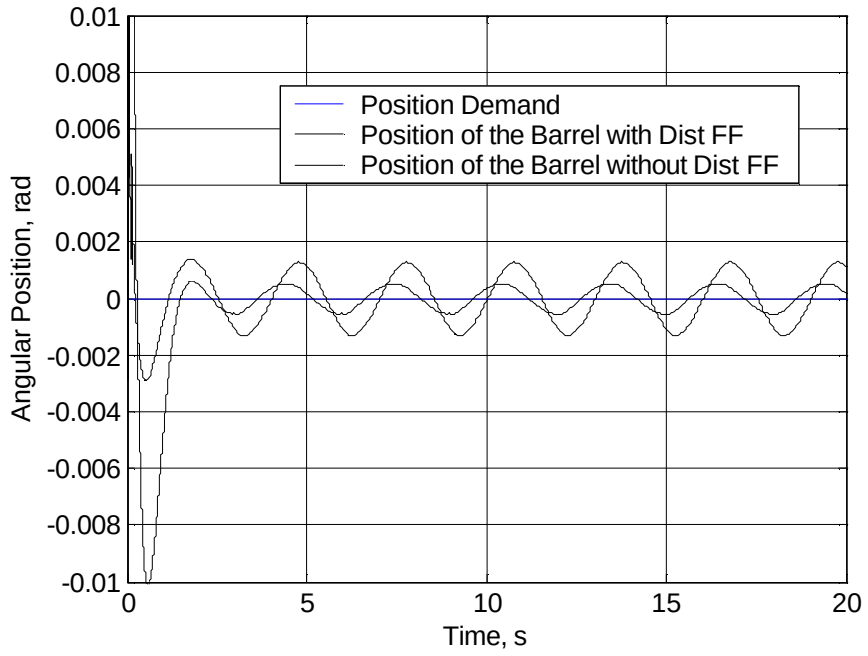

Figure 54. Position of the Barrel with Disturbance FF with a Velocity of

V=20 km/h

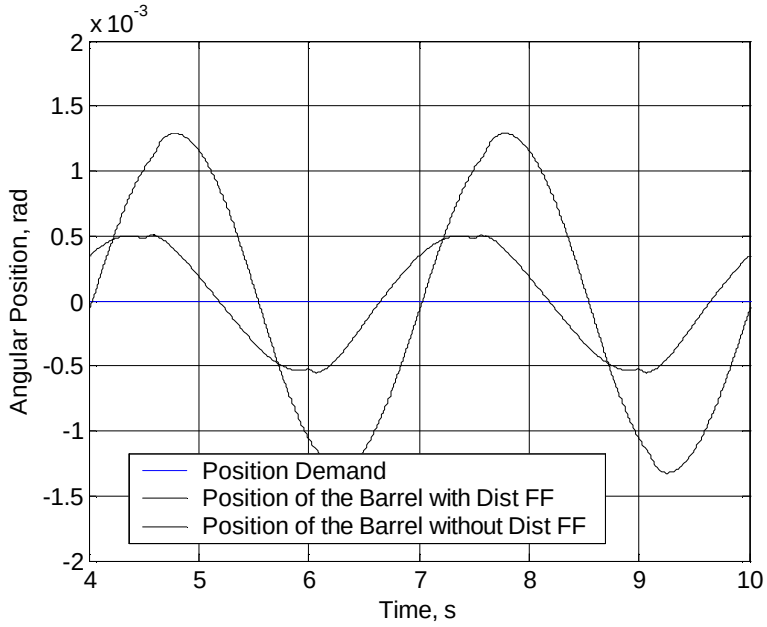

Figure 55. Zoomed View of Figure 54

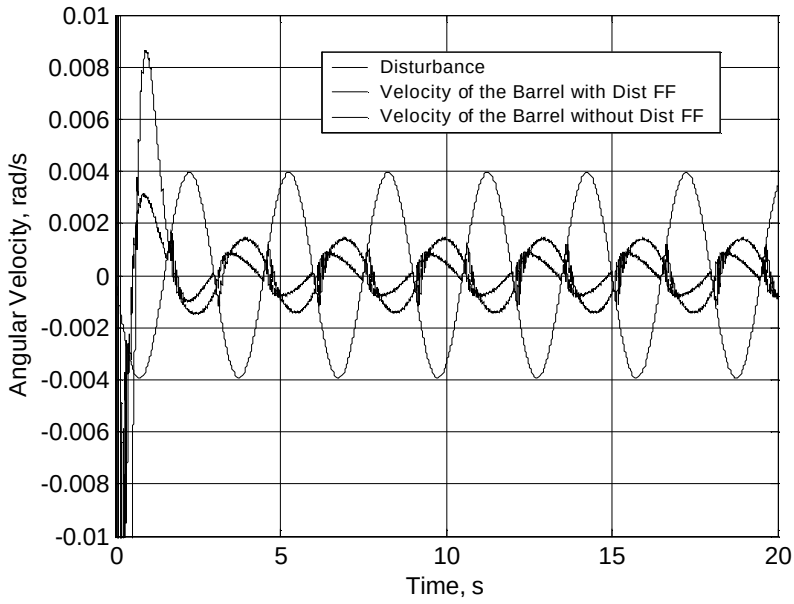

Figure 56. Disturbance and Effect Disturbance FF with a Velocity of V=40 km/h

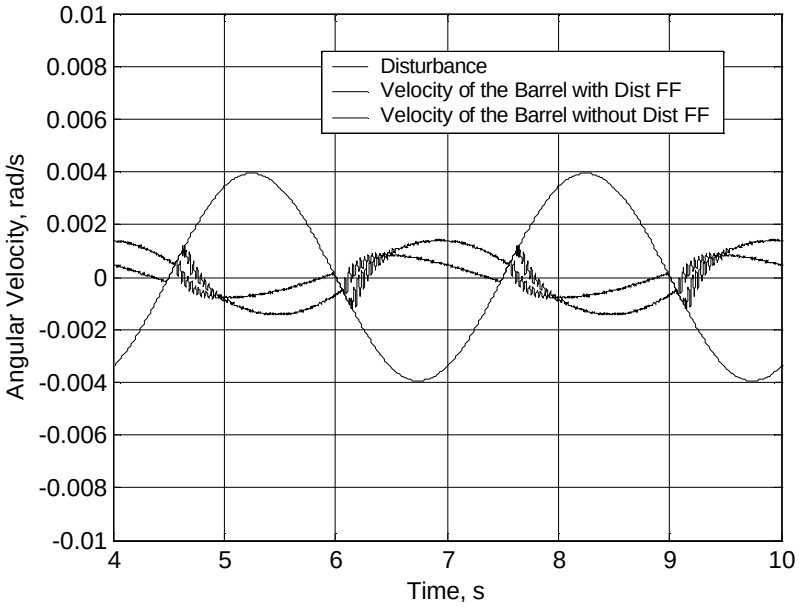

Figure 57. Zoomed View of Figure 56

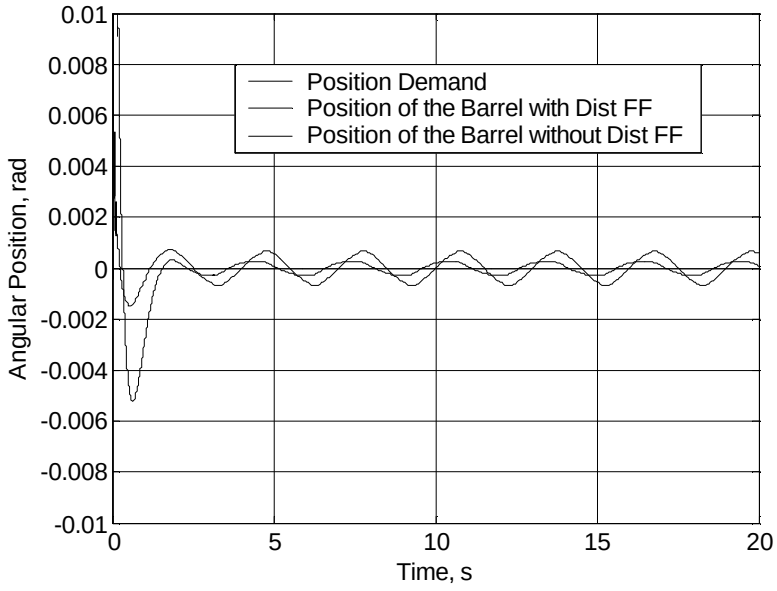

Figure 58. Position of the Barrel with Disturbance FF with a Velocity of V=40 km/h

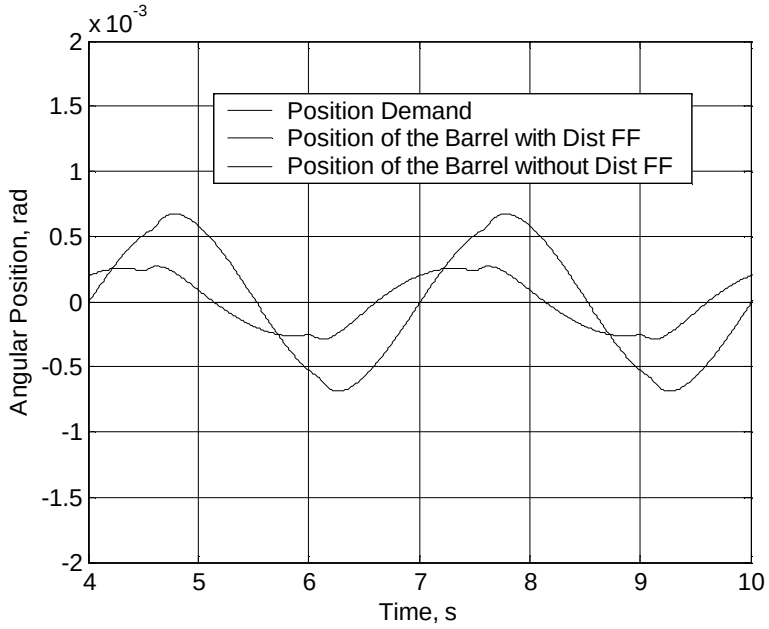

Figure 59. Zoomed View of Figure 58

The position and the velocities of the barrel for two cases explained before can be seen in the figures from Figure 53 to Figure 60. The deviation of the barrel position from the zero point is differing but the best ones are the cases in which the disturbance feed forwards are used. Stabilization accuracy is about $1x10^{-3}$ rad while the V=20 km/h and $\omega_d = 0.016$ rad/s and $6x10^{-4}$ while the V=40 km/h and $\omega_d = 0.008$ rad/s. The minimum stability accuracy determined in [3] with basic, second generation and director type stabilization systems is 1.0 mil, 0.5 mil and 0.2 mil respectively. While a circle is 6280 milirad or 6400 mil, stabilization accuracy of the model will be equal to 0.1 milirad or 0.102 mil. Compare to these values, model has an accuracy same as the basic stabilization system.

CHAPTER 5

CONCLUSION

5.1. Summary and Conclusion

In this study, stabilization of a Main Battle Tank is considered. System elements are examined one by one and modeled in Matlab® Simulink® environment. Modeling is a difficult problem itself and to be able to model the systems assumptions for undetermined facts and nonlinearities must be done. System controller, electrohydraulic servo valve, actuating system (slider-crank mechanism), barrel are elements of the Main Battle Tank system.

Control system is constructed by using PID controllers. Velocity feed forward is used to make the system more rapid. It has two PID controllers one for position loop and the other for the velocity loop. Disturbances which come from the ground via the hull were embedded to the system from the control signal to make the system more sensitive to the changes in hull motion. Stabilization, disturbance rejection, is tried to be improved by adding disturbance compensation. The transfer function between the disturbance and the output of the system is determined. Frequency response is examined and the contents of the feed forward strategy are determined.

Servo valve is a zero-lapped, classical four way valve. It has three stages. The valve is modeled as second order system. Valve dynamics are identified by the help of the actual system's step response records. Simulations and comparisons with the actual system are made with the model parameters found with identification. Nonlinearity in the servo valve is considered.

Actuation system is a double-acting hydraulic cylinder coupled with a slider-crank mechanism which transforms the translational motion to the rotational. Inverse kinematics is considered in the solution while modeling. The cylinder and the pressurized lines are assumed to be absolutely rigid. Compressibility in the actuation system is considered. Piston areas are equal in the system but it is considered that they may be different for other systems while modeling.

Angular position of the barrel is the output of the system. Inertial effects, Coulomb and viscous frictions, hard-stops define the motion of the barrel. A simplified model of the barrel is constructed to define the possible cases with the effects of inertia, friction and hard-stops. The way of effecting of disturbance caused from the road profile is as an angular velocity at the joint which mounts the barrel to the hull. The source of this velocity, acceleration and unbalance affect the barrel in vertical axis.

The measurement devices used in the actual systems are also modeled. These are LVDT in servo valve, gyroscopes on the hull and gyroscope and encoder on the barrel. LVDT is represented in the system model as a gain, gyroscope as a second order transfer function and encoder as a quantization block.

Simulations are made for the stabilization system. They are made with two different constant velocities but the model can also solve the situation with variable velocities.

Model which was constructed for Main Battle Tank gives the opportunity to use any of the elements included in the system without risk of hazard for machines and users separately. Also, they can be used to design the possible future systems.

5.2. Recommendations for Future Work

System modeled in this study will be satisfactory to examine the main cases included and will be helpful for users. For future work, other probable components can be added to the model such as pipes, hydraulic fluid temperature, leakage etc.

PID controllers are very common in industry. However, there is not a common method for tuning these controllers. PID controllers are dominant, effective, simple and applicable for all kinds of systems. Other controller strategies may be tried such as intelligent control, full state feedback etc.

Hull dynamics is neglected in this study and output of the hull gyro is used directly. Hull model may be constructed and actual road profiles may be used.

The servo valve is identified in this study with very limited data. A better valve can be used or may be done additional tests on the valve to make a better model of the servo valve.

Coulomb and viscous frictions are modeled but it is assumed that they exist only in the joint which mounts the barrel to the hull. The other mountings such as the one between the piston and the barrel and the one between the cylinder and the hull, actuation system have also frictions.

REFERENCES

[1] **Şahin, S., (2001),** “Stabilization and Orientation of Tank Gun”, M.S. Thesis, METU Mechanical Engineering Department, Ankara.

[2] **Ogorkiewicz, R. M., (1991),** “Technology of Tanks”, Vol.1, Jane’s Information Group Limited.

[3] **Ogorkiewicz, R. M., (1978),** “Stabilised Tank Gun Controls”, International Defense Review, pp. 725-728.

[4] **Balaman, M. R., (1984),** “Time Optimal Control of a Manipulator with Two Angular Degrees of Freedom”, METU Mechanical Engineering Department, Ankara.

[5] **Purdy, J. D., (1998),** “Main Battle Tank Stabilization Ratio Enhancement Using Hull Rate Feed Forward”, Journal of Battlefield Technology, Vol. 1, No. 2, pp. 5-9.

[6] **Purdy, J. D., (1999),** “On the Stabilization of Out-Of-Balance Guns”, Journal of Battlefield Technology, Vol. 2, No. 3, pp. 1-7.

[7] **Batu, U., Gürcan, M. B., Balkan, T.,** “Hidrolik Servo Valflerin Dinamik Modelleri ve Performans Testleri”, III. Ulusal Hidrolik Pnömatik Kongresi ve Sergisi, 4-7 Aralýk 2003, Ýzmir, pp. 13-26.

[8] **De Boer, C. C., Yao, B., (2001),** “Velocity Control of Hydraulic Cylinders with Only Pressure Feedback”, Proceedings of IMECE’01, ASME, 11-16 November 2001, New York.

[9] **Thayer, W. J., (1965),** “Technical Bulletin I03”, MOOG Inc. Control Division, East Aurora.

[10] **Çelik, M., Aykan, M., (2004),** “Tank Namlusunun Operasyonel ve Deplasman Analizi”, Makine Tasarým ve Ýmalat Dergisi, Cilt 6, Sayý 1, pp. 50-57.

[11] “Electronic Control of Hydraulic Systems”, Electronics in the Mobile Equipment Industries, Technical Documents, HYDRAFORCE Inc., http://www.hydraforce.com/Electro/Elec-pdf/3-561-1.pdf, Last Update, 07.12.2004

[12] Harb, S. M., (1985) “Experimental Investigation of the Performance Improvement of Slowly Moving Fluid Power Drives via Dither Produced by Pulse Width Modulation”, METU Mechanical Engineering Department, Ankara.

[13] “Electrohydraulic Valves… A Technical Look”, MOOG Inc. Control Division, East Aurora., http://moog.com/Media/1/technical.pdf, Last Update, 07.12.2004

[14] Ercan, Y., (1995), “Akýþkan Gücü Kontrol Teorisi”, Gazi Üniversitesi Yayýnlarý.

[15] Papaopoulos, E. G., Chasparis, G. C.,(2002) “Analysis and Model-Based Control of Servomechanisms with Friction”, Proceedings of the International Conference on Intelligent Robots and Systems (IROS 2002), Lausanne, Switzerland. 2-4 October 2002.

[16] Gayakwad, R., Sokoloff, L., (1998), “Analog and Digital Control Systems”, Prentice Hall.

[17] Marlin, T. H., (1995), “Process Control”, 2nd Ed., McGraw Hill.

[18] Ellis, G., (2000), “Feed Forward in Position Velocity Loops”, 20-Minute Tune-Up, PT Design Magazine, September 2000, pp. 68-70.

[19] Ellis, G., (1999), “Closing a PID Velocity Loop”, 20-Minute Tune-Up, PT Design Magazine, February 1999, pp.29-31

APPENDIX 1

VALVE IDENTIFICATION

Matlab “m” file developed for the valve identification is as follows.

```
% Valve Identification;
% Two test results used at each amplitude

clear all; clc
load datak.mat
valtp=datak(:,2:2);
ti=[0.001:0.001:1];
error=10;

TD=[valtp(14001:15000,:) valtp(18001:19000,:)...
    valtp(12001:13000,:) valtp(16001:17000,:)...
    valtp(22001:23000,:) valtp(30001:31000,:)...
    valtp(28001:29000,:) valtp(32001:33000,:)...
    valtp(37001:38000,:) valtp(41001:42000,:)...
    valtp(36001:37000,:) valtp(40001:41000,:)...
    valtp(51001:52000,:) valtp(59001:60000,:)...
    valtp(52001:53000,:) valtp(56001:57000,:)];

figure
plot(ti,TD)
xlabel('Time,sec')
ylabel('Valve Position,mm')
figure
plot(datak(:,1:1),datak(:,3:3)*10/6.5)
xlabel('Time,sec')
ylabel('Input Voltage,V')
figure
plot(datak(:,1:1),datak(:,2:2)*10/6.5)
xlabel('Time,sec')
ylabel('Valve Position,mm')

x_max= 7.0             ;  % Maximum spool stroke, mm
LVG         = 10/6.5         ;  % LVDT Gain, V/mm

Test=[0.25 0.25 -0.25 -0.25 0.5 0.5 -0.5 -0.5 1 1 -1 -1 2 2 -
2 -2]           ;  % Test Input

G=[21:0.1:23]        ;    % Gain Search Matrix
z=[0.002:0.0002:0.004]    ;    % Time Search Matrix
```

```
for i=1:21
    K=G(i)

    for a=1:11
        T=z(a);
        ee=0;
        for p=1:12
            I=Test(1,p);
            TDG=TD(:,p:p)';

            st=2;   % step time=1 and duration 1 sec in
simulation
            [t,x,yout]=sim('scndstage');
            yot=(yout(1001:2000,:))';
            e=sum((yot-TDG).^2);
            ee=ee+e;
        end
        e1(i,a)=ee/12
        if e1(i,a) < error
            error=e1(i,a);
            ii=i;
            aa=a;
        else
        end
    end
end

figure
surf(z,G,e1)
xlabel('Time,sec')
ylabel('Gain')
zlabel('Error')

for p=13:16
    I=Test(1,p);
    st=2;   % step time=1 and duration 1 sec in simulation
    K=G(ii);
    T=z(aa);
    TDG=TD(:,p:p)';
    [t,x,yout]=sim('scndstage');
    yot=(yout(1001:2000,:))';
    figure
    plot(ti,yot)
    hold
    plot(ti,TDG,'m')

end

K,T
```

APPENDIX 2

FRICTION MODEL AND RESULTS

This Matlab “m” file developed for the simplified barrel model.

```
%  To plot different scenarios for the friction model
% First Column Torque apllied from outside
% Second Column Frequency of the Output Torque
% Third Column Disturbance Torque
% Fourth Column Frequency of Disturbance Torque

TFDF=[1     1       0       1
      1.1   1/6     0       1
      1.1   1/4     0       1
      1.5   1/4     0       1
      1.1   1/2     0       1
      1.5   1/2     0       1
      0     1       1       1/5
      0     1       1.2     1/5
      0     1       0.4     1/3
      0     1       0.6     1/3
      0     1       0.7     1/3
      0     1       0.8     1/3]

for i=1:14
    T=TFDF(i,1);
    Tf=TFDF(i,2);
    D=TFDF(i,3);
    Df=TFDF(i,4)
    [t,x]=sim('frict0510_limitli_2fric_t.mdl');
    load w.mat;
    load th.mat;
    v=w';
    the=th';
    figure;
    subplot(211),plot(v(:,1:1),v(:,2:3)),grid
    title('Velocity Plot')
    ylabel('Angular Velocity,Rad/sec')
    subplot(212),plot(the(:,1:1),the(:,2:4)),grid
    title('Position Plot')
    xlabel('Time,sec')
    ylabel('Angular Position,Rad')
end
```

Some of the simulation results are revealed in Chapter 4 and rest of the friction simullation results can be plotted as follows for different situations.

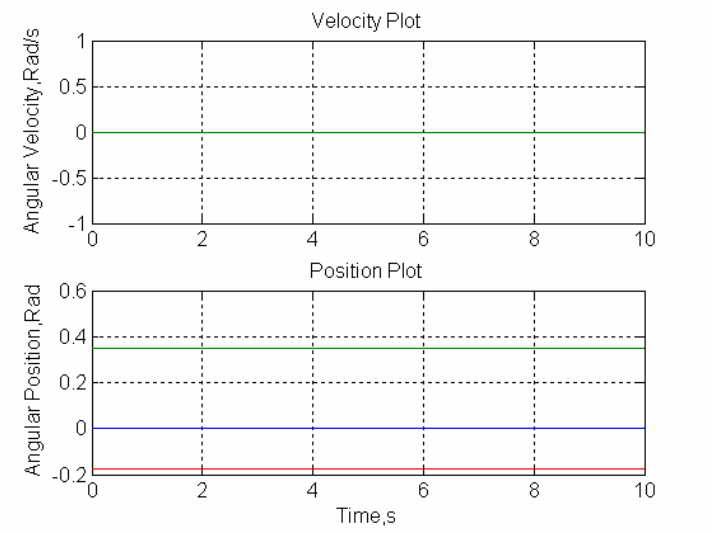

Figure A.1. Velocity and the Position of Simplified Barrel

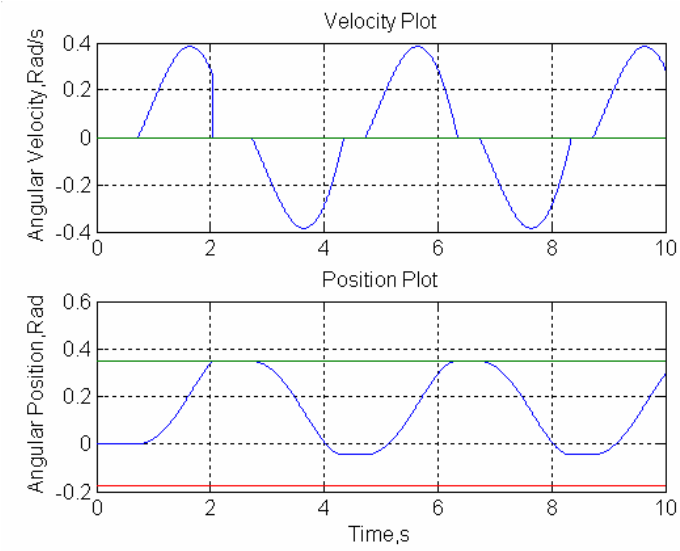

Figure A.2. Velocity and the Position of Simplified Barrel

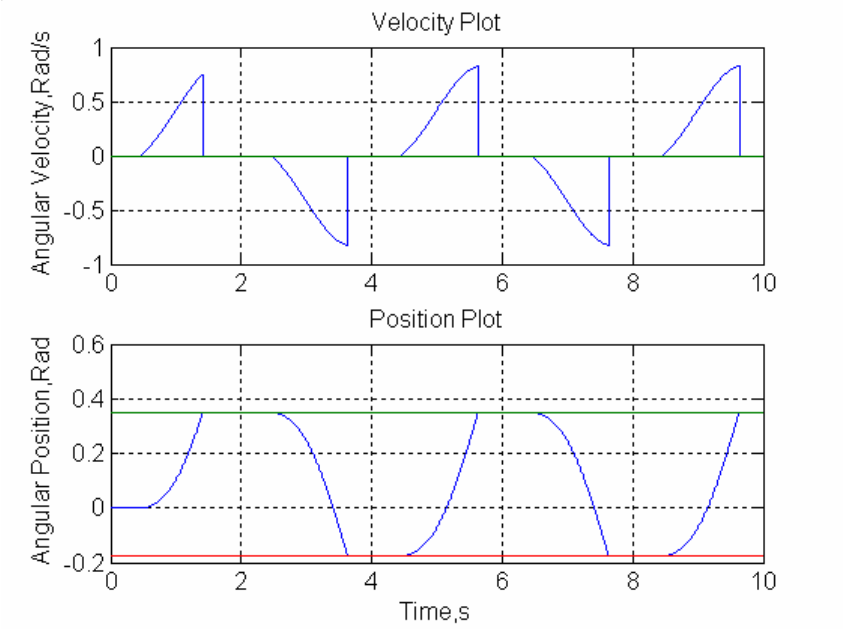

Figure A.3. Velocity and the Position of Simplified Barrel

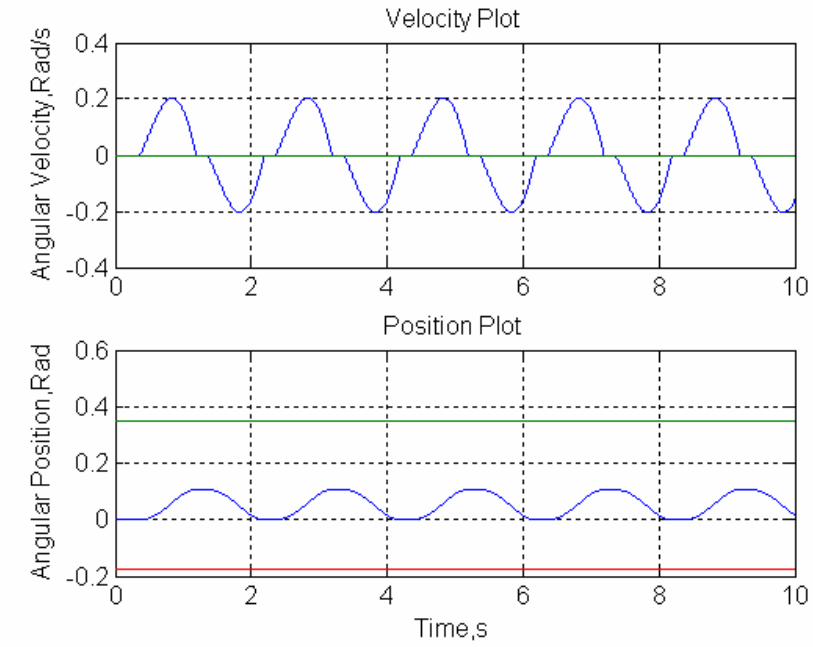

Figure A.4. Velocity and the Position of Simplified Barrel

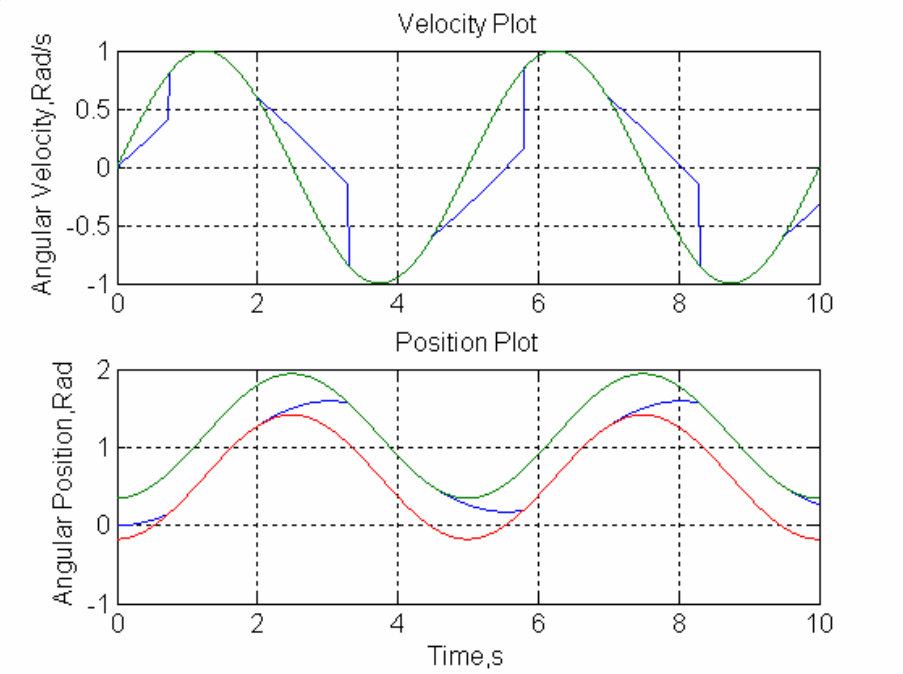

Figure A.5. Velocity and the Position of Simplified Barrel

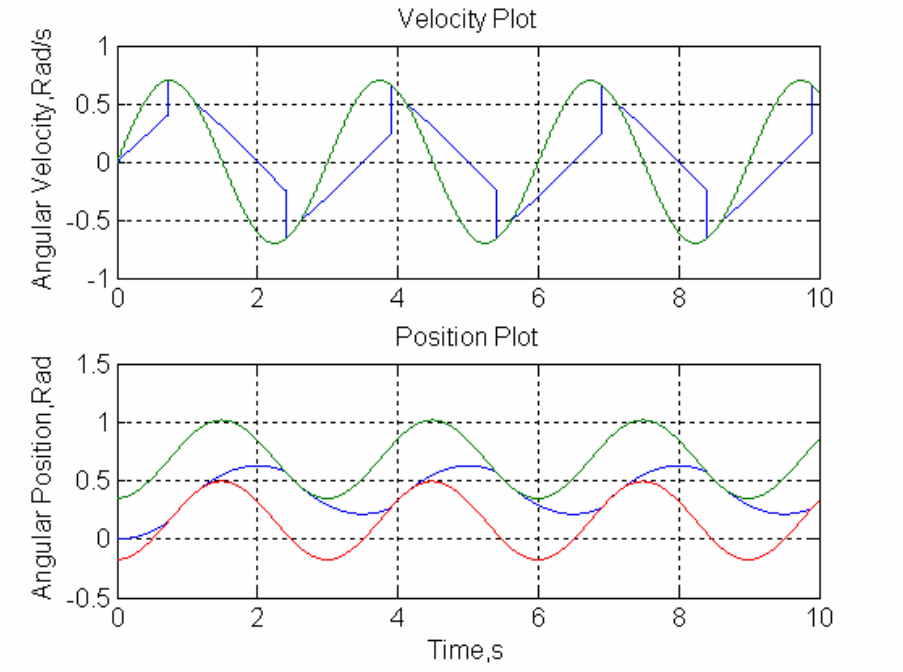

Figure A.6. Velocity and the Position of Simplified Barrel

APPENDIX 3

PARAMETERS

This “m” file is developed for the defining the parameters used in the stabilization system model.

```
% Parameters for Barrel Model
clear all; clc

g      = 9.81   ;  % Gravitational acceleration (m/s2)
t_st   = 5e-4     ;  % Time Step of The Solution

% Hydraulic System Parameters
pS   = 70e5     ;    % Supply pressure, Pa
beta   = 1.72e9   ;  % Bulk modulus of oil, Pa (250,000 psi)
d_oil  = 890    ;  % Oil density, kg/m3
Cd     = 0.625    ;    % Orifice Discharge Coefficient


% Inverse Kinematics
a      = 0.44     ;    % Slider Krank Length, m
r      = 1.05     ;    % Slider Krank Length, m


% Valve Dynamics
K      = 21.8     ;    % Valve Gain, mm/V
T      = 0.003    ;    % Valve Time Constant, s
x_max  = 7.0      ;    % Maximum spool stroke, mm

% Flow Characteristics
va_op  = 6.5e-3 ;    % Maximum valve opening, m
wo    = 2*1.24e-3  ;  % Width of orifice, m
KV    = Cd*wo*sqrt(2/d_oil);  % Orifice gain
(m2/(s.sqrt(Pa)))
LVG    = 1        ;  % LVDT Gain, V/mm
% Actuator & Slider Crank
d_o_a  = 0.07   ;    % Cylinder diameter, m
d_i_a  = 0.032  ;    % Piston shaft diameter, m
Aa  = pi*(d_o_a^2-d_i_a^2)/4 ; % Piston area, m2

d_o_b  = 0.07   ;  % Cylinder diameter, m
d_i_b  = 0.032  ;    % Piston shaft diameter, m
Ab   = pi*(d_o_b^2-d_i_b^2)/4 ;   % Piston area, m2
```

```
yp_max = 0.2 ;    % Maximum piston stroke length, m
ypc_max= 0.198    ;  % Cylinder off-set
ypc_min= 0.002    ;  % Cylinder position
y_c    = 0.7    ;  % Cylinder offset, m

dd     = 2e-3     ;  % Dead Part's Length, m

% Barrel
m      = 250      ;  % Barrel's weight, kg
Jg     = 500      ;  % Mass Moment of Iner. of the Barrel,
kgm2
V_Vfr  = 0.2      ;  % Viscous Friction

Frload = 10.73    ;  % Load Critical Frequency
Tfb    = 1/(Frload/3)  ;  % HP Filter Time Constant
LPFB   = 1e-7   ;  % Presssure Transducer Gain, V/MPa

the_max= pi/9     ;  % Barrel's Maximum Limit, degree
the_min= -pi/18   ;  % Barrel's Minimum Limit, degree

Vv     = 11.12  ;  % Vehicle's Vel, m/sec , 20 km/h=5.56 m/s
lambda = 100    ;  % Wave length of Raod Profile, m
le     = 0.1    ;  % Off-Set from the road, m
lg     = 0.25   ;  % Unbalance Moment Leg, m

% Gyroscpe
wn     = 30*2*pi  ;  % Natural Frequency
z      = 0.707  ;  % Damping Ratio

Gy_n=[wn^2]     ;  % Numerator of the Gyroscopes
Gy_d=[1 2*wn*z wn^2] % Denominator of the Gyroscopes

Dffn=[0.08469 18.92 796.8 36100]  ;  %Numerator of the Dist FF
Dffd=[0.001388 2.015 781 35360]   ;  %Denominator of the FF
```